Thermodynamic and Kinetic Basis of Interfacial Activation: Resolution of Binding and Allosteric Effects on Pancreatic Phospholipase A_2 at Zwitterionic Interfaces[†,‡]

Otto G. Berg,[§] Joseph Rogers,[||] Bao-Zhu Yu,[||] Jihu Yao,[⊥] Laurence S. Romsted,[⊥] and Mahendra Kumar Jain*[,||]

Department of Chemistry and Biochemistry, University of Delaware, Newark, Delaware 19716, Department of Chemistry, Wright and Rieman Laboratories, Rutgers, The State University of New Jersey, New Brunswick, New Jersey 08903, and Department of Molecular Biology, Uppsala University Biomedical Center, Uppsala, Sweden

Received April 14, 1997; Revised Manuscript Received September 8, 1997[⊗]

ABSTRACT: A general kinetic model for catalysis by interfacial enzymes is developed. It couples the Michaelis−Menten catalytic turnover cycle at the interface with that in the aqueous phase through the distribution equilibria between the interface and the surrounding aqueous phase. Analysis under two limiting conditions fully describes the steady-state kinetics of hydrolysis and resolves the allosteric effects from apparent modes of interfacial activation in terms of the primary rate and equilibrium parameters for pig pancreatic phospholipase A_2 (PLA2). One limit is observed in dispersions of anionic phospholipid vesicles, in which intervesicle exchange of enzyme, substrate, and hydrolysis products is absent and reaction occurs only on vesicles containing enzyme. A complete analysis at this highly processive limit, called kinetics in the scooting mode, has been published [Berg et al. (1991) *Biochemistry 30*, 7283]. Here is reported the analysis in the other limit, PLA2-catalyzed hydrolysis of zwitterionic micelles of short-chain phosphatidylcholines, at which substrate and products are in rapid exchange. Hydrolysis occurs either in bulk aqueous solution with phospholipid monomers or at the micellar interface. Above the critical micelle concentration (cmc), the hydrolysis rate shows a hyperbolic dependence on the bulk substrate concentration present as micelles. This dependence, characterized by the fitting parameters K_M^{app} and V_M^{app}, is analyzed in terms of the primary rate and equilibrium constants. The kinetic analysis is based on the assumption that the microscopic steady-state condition is satisfied because substrate replenishment in the microenvironment of the enzyme is fast relative to the catalytic turnover time. Added NaCl and anionic interface increase the hydrolysis rate in zwitterionic micelles dramatically. The overall interfacial rate enhancement is attributed to three factors: (a) promotion of PLA2 binding by net anionic charge of the interface, (b) enhancement of substrate affinity of PLA2 at the interface (K_S* allostery), and (c) stimulation of the rate-limiting chemical step (k_{cat}* allostery).

T. S. Elliot observed: "... and the end of all our exploring will be to arrive where we started and know the place for the first time".

More than 25 years ago de Haas et al. (1971) reported the substrate concentration dependence of pig pancreatic phospholipase A_2 (PLA2)[1] catalyzed hydrolysis of short-chain phosphatidylcholines. The rate of hydrolysis increases above the cmc, and the increase depends on the NaCl concentration. In conjunction with earlier studies [reviewed in Jain et al. (1973)] these observations provided the grail for exploring PLA2 as a prototype for interfacial enzymology (Verger & de Haas, 1976; Verheij et al., 1981; Dennis, 1983; Waite, 1987; Jain & Berg, 1989; Gelb et al., 1995). We formulate the collective experience of PLA2-catalyzed phospholipid hydrolysis as Scheme 1, a general kinetic model for interfacial catalysis. The experimental focus of this paper and the general theory and kinetic predictions of the model are analytically derived in the Appendix for the fast exchange limit at which the catalytic turnover remains rate limiting under conditions when substrate and product exchange is not limiting. Besides providing a rigorous framework for the interpretation of the substrate, inhibitor, and cofactor dependence, this analysis permits unequivocal separation of

[†] Dedicated to Eugene Cordes for introducing M.K.J. and L.S.R. to the fascinating complexities of interfaces, enzymes, and catalysis.

[‡] This work was supported by the PHS (GM29703 to M.K.J.), NSF (95-26206 and U.S. Latin American Cooperative Program-Brasil to L.R.), and Swedish Natural Science Research Council (to O.B.). J.Y. was supported by the Center for Food Technology.

* Author to whom correspondence should be addressed (e-mail mkjain@udel.edu).

[§] Uppsala University Biomedical Center.

[||] University of Delaware.

[⊥] Rutgers University.

[⊗] Abstract published in *Advance ACS Abstracts,* November 1, 1997.

[1] Abbreviations: 16-ArN_2BF_4, 4-hexadecyl-2,6-dimethylbenzenediazonium tetrafluoroborate; 16-ArN_2^+, 4-hexadecyl-2,6-dimethylbenzenediazonium ion; 16-Ar^+, 4-hexadecyl-2,6-dimethylphenyl cation; 16-ArOH, 4-hexadecyl-2,6-dimethylphenol; 16-ArCl, 4-hexadecyl-2,6-dimethylchlorobenzene; cmc, critical micelle concentration defined in Scheme 1 as the distribution constant for the substrate (K_S') or a substrate mimic (K_I') such as a competitive inhibitor; DC$_n$PC, 1,2-diacylglycero-*sn*-3-phosphocholine with *n* carbons in each chain; DC$_n$PC-ether, 1,2-dialkylglycero-*sn*-3-phosphocholine with *n* carbons in each chain; DC$_n$PM, 1,2-diacylglycero-*sn*-3-phosphomethanol; deoxy-LPC, 1-hexadecylpropanediol-3-phosphocholine; DTPC, 1,2-ditetradecylphosphatidylcholine; I, an active-site-directed substrate mimic or a competitive inhibitor; MG14, L-1-*O*-octyl-2-heptylphosphonyl-*sn*-*glycero*-3-phosphoethanolamine; MJ33, 1-hexadecyl-3-(trifluoroethyl)-*rac*-*glycero*-2-phosphomethanol; MJ72, 1-octyl-3-(trifluoroethyl)-*rac*-*glycero*-2-phosphomethanol; PLA2, phospholipase A_2 from pig pancreas unless indicated otherwise; PNBr, *p*-nitrophenacylbromide (2-bromo-4′-nitroacetophenone); POPC, 1-palmitoyl-2-oleoyl-*sn*-3-glycerophosphocholine; RM3, 1-thiooctyl-2-acetamido-*sn*-propyl-3-phosphocholine; TMACl, tetramethylammonium chloride. Definitions of the primary rate and equilibrium constants are shown in Scheme 1, and their relationships to apparent parameters are developed in the Appendix.

S0006-2960(97)00855-6 CCC: $14.00

Scheme 1: General Kinetic Model for Interfacial Catalysis under Conditions in Which the Enzyme, Substrate, Products of Hydrolysis, and Inhibitor Are Distributed between the Aqueous Phase and the Interface[a]

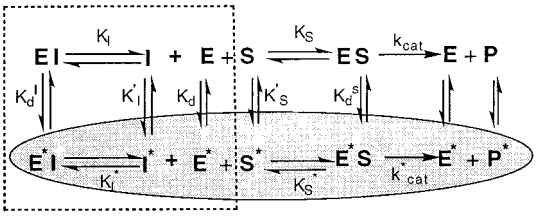

[a] The Michaelis rate parameters at the interface (marked with an asterisk) and the aqueous phase (without an asterisk) are defined according to standard nomenclature. Enzyme-mediated catalytic turnover occurs at the interface (through E* and E*S) and through the decomposition of solitary ES complex. The steps shown in the oval describe catalytic turnover at the interface (Berg et al., 1991). The rate-limiting steps, k_{cat} and k_{cat}* are the rate constants for decomposition of ES and E*S, respectively. The detailed balance condition relating the equilibria in the square box provides the quantitative thermodynamic basis (eqs 5 and 6) for the equilibria on aggregate surfaces and in bulk aqueous solutions (Jain et al., 1993b). A general term, I, in the text denotes substrate mimics including active site directed competitive inhibitors (I) or the products of hydrolysis (P). The equilibrium dissociation constants (for example, K_d^I, K_I', K_d, K_S', K_d^S) are for the species related by double arrows and are written using standard definitions (Jain et al., 1995).

the observed kinetic effects of surface charge and other variables that control the binding of PLA2 to the interface, as well as other interfacial exchange processes (vertical arrows in Scheme 1), from the allosteric effects on the interfacial substrate binding or the chemical step of the two catalytic cycles (horizontal arrows).

Catalysis Occurs at the Interface. Key results and concepts leading to the analysis of the general kinetic model for interfacial catalysis and activation merit a brief review, which should also serve as a primer for the versatility of Scheme 1. Early evidence for the assertion that enhanced catalytic turnover by PLA2 occurs at the interface (de Haas et al., 1971; Jain and Cordes, 1973; Dennis, 1973; Verger et al., 1973) was circumstantial. Explicit evidence for catalytic turnover at the interface (shaded oval in Scheme 1) was unequivocally established with the demonstration of the highly processive interfacial kinetics in the scooting mode (Jain et al., 1986a−c, 1995). Under these conditions PLA2 is tightly bound to the anionic vesicle surface and cleaves all phospholipid on the exo surface (Berg et al., 1991). The reaction ceases when all substrate on the enzyme-containing vesicle is hydrolyzed because bound enzyme does not transfer to unhydrolyzed vesicles in the reaction mixture (Jain et al., 1991c). Vesicle integrity is retained because substrate and product molecules do not transfer between vesicles or across the bilayer (Yu et al., 1997).

An appreciation of the differences in microscopic steady-state condition in micellar and vesicular solutions is critical for interpreting interfacial catalysis. Kinetic analysis requires summation of individual steps in the reaction pathway. This is possible only when all enzyme molecules in the ensemble "see" the same average microenvironment at any given point in the progress of the reaction (Berg et al., 1991). Because PLA2 bound to anionic vesicles does not exchange in the processive scooting mode, the summation over the whole population is possible for the hydrolysis by using a Poisson excess of vesicles of narrow size dispersity such that at most one enzyme molecule is present on each enzyme-containing vesicle. This permits determination of the interfacial rate and equilibrium parameters (Berg et al., 1991; Yu et al., 1993, 1997).

A useful concept for interfacial catalysis is that the binding of the enzyme to the interface (E to E*) and the binding of the substrate to the enzyme at the interface (E* + S* to E*S) are separate events. This difference is structurally conceptualized as the interfacial recognition region and the active site, respectively (Verger & de Haas, 1976; Verheij et al., 1981). Thus, a critical first step for resolving the two-dimensional rate and equilibrium constants (Berg et al., 1991) is to identify a neutral diluent (Jain et al., 1991a): PLA2 binds to aqueous dispersions of a neutral diluent, such as deoxy-LPC; however, deoxy-LPC does not bind to the active site of the enzyme at the interface. Thus, diluents permit determination of K_d for E $\rightleftarrows$ E*, K_I* for E* + I* $\rightleftarrows$ E*I, and virtually all parameters required for the analysis of interfacial catalysis (Jain et al., 1991a,b; Yu et al., 1997).

The primary rate and equilibrium parameters for the interfacial catalytic turnover cycle of PLA2 have provided useful insights (Jain et al., 1995). The chemical step is rate limiting during the processive catalytic turnover at anionic vesicular interface (Jain et al., 1992). Calcium is an obligatory cofactor for the binding of active-site-directed mimics (S or I) and for the chemical step of the catalytic cycle but not for the binding of the enzyme to the interface, the E to E* step (Yu et al., 1993; Li et al., 1994). For example, studies with site-directed mutants have shown that Tyr-52, Phe-22, and Phe-106 participate in substrate binding (Dupureur et al., 1992a,b); that Asp-99 affects k_{cat}* (Sekar et al., 1997); that the N-terminal residues contribute to the binding of the enzyme to the interface (Maliwal et al., 1994; Liu et al., 1995); and that the C-terminal segment participates in coupling of the chemical step to the anionic charge at the interface (Huang et al., 1996). Scheme 1 also accommodates kinetics with anionic micelles, where PLA2 binds with high affinity, substrate exchange with excess micelles is rapid, and the catalytic turnover is limited by the chemical step (Jain & Rogers, 1989; Rogers et al., 1996). Also, direct vesicle to vesicle exchange of phospholipid mediated by peptides and proteins provides a kinetic basis for rationalizing nonspecific inhibition (Jain & Berg, 1989) and the apparent activation of PLA2 under conditions leading to increased substrate replenishment (Jain et al., 1991c; Cajal et al., 1996a,b, 1997; Cajal & Jain, 1997).

Finally, kinetic analysis based on Scheme 1 also provides a basis for understanding interfacial activation in terms of the primary processes. For example, the five distribution equilibria for the interaction of PLA2 with the interface and with a substrate mimic constitute a "thermodynamic box", marked by a square on the left side of Scheme 1. These equilibria are related by a detailed balance condition, eq A4 (all equations with the prefix A are in the Appendix), which permits comparison of equilibrium constants with different dimensionality. K_I (moles per liter) and K_I* (mole fraction) values for several mimics show that their intrinsic affinity for PLA2 is about 50-fold higher at the interface than it is in the aqueous phase (Jain et al., 1993b). These results suggest that the interface is a K_S*-allosteric activator, and results in this paper show that the anionic charge at the interface increases k_{cat}*.

Scope of This Paper. As developed in this paper, according to Scheme 1, microscopic steady state for the

hydrolysis of micelles of short-chain phosphatidylcholines by PLA2 can be achieved in the limit of rapid exchange of substrate and products; that is, a quasiequilibrium is established between the micelle and the surrounding aqueous phase if the substrate replenishment and product desorption are faster than the interfacial catalytic turnover. Thus, PLA2-catalyzed hydrolysis of anionic vesicles in the scooting mode and that of zwitterionic micelles by rapid exchange represent two limits for Scheme 1, at which exchange rates of substrate, products, and enzyme between aggregates and bulk aqueous phase do not affect the observed kinetics, albeit for very different reasons. The key point is that in both cases the microscopic environment of *all* the enzyme molecules in the reaction mixture remains the same and unchanged during the course of the steady-state reaction progress and the catalytic turnover is rate limiting. Departure from microscopic steady-state condition is not uncommon (Jain et al., 1995; Nelsestuen & Martinez, 1997), and the exchange-limited kinetics are observed with PLA2 assays involving monolayers (Jain & Berg, 1989) and mixed micelles (Jain et al., 1993a). Results of exchange-limited assays are not readily amenable to analysis in terms of the primary rate and equilibrium constants of the catalytic turnover cycle.

To support our assertion that Scheme 1 constitutes a general kinetic basis for interfacial catalysis and activation, we revisit the original observations of de Haas et al. (1971) on the PLA2-catalyzed hydrolysis of zwitterionic DC_nPC ($n = 6-8$) in micellar aqueous dispersions. In agreement with earlier suggestions (Pieterson et al., 1974; Verger & de Haas, 1976; Roberts et al., 1977; Verheij et al., 1981; Dennis, 1983), two pathways exist in Scheme 1 for catalytic turnover in the aqueous phase and the interface, and contributions from both branches describe the observed rate. k_{cat} of the upper branch describes turnover via decomposition of monodisperse ES in the aqueous phase, and k_{cat}* of the lower branch (shaded oval) is via the interfacial Michaelis complex, E*S. Experimental results are developed in three stages. First, we characterize the hyperbolic bulk micellar substrate concentration dependence of the observed rate in the presence and absence of added NaCl in terms of K_M^{app} and V_M^{app}. In the second part we show that the dependence of K_M^{app} on NaCl concentration is due to selective partitioning of chloride ion into zwitterionic interface, giving the interface a net negative charge. In the last part we analyze the effect of added NaCl on the equilibria related by the detailed balance condition (square box in Scheme 1) and show that the NaCl-induced increase in the V_M^{app} is caused by an increase in k_{cat}*. In short, a complete set of primary constants is now available for the analysis of interfacial catalysis by PLA2.

Experimental Strategy and Key Results. We show that the steady-state kinetics of hydrolysis of DC_nPC ($n = 6-8$) micelles are described by a single set of primary rate and equilibrium constants in the limit of rapid substrate replenishment so that the catalytic turnover is rate limiting. Equations 5 and 6 (A3 and A4) relate five equilibrium dissociation constants that control individual branches for the steady-state fluxes. These expressions are free of concentration-dependent terms in the bulk aqueous phase and at the two dimensional interface. In the complete thermodynamic cycle (square box in Scheme 1), all concentration terms disappear and the units for each branch cancel out. Assuming that the catalytic turnover is rate limiting, the steady-state rate of hydrolysis is given by a unified expression in the presence (eq A5) or absence (eq A6) of competitive inhibitors. Values of K_M^{app} and V_M^{app} obtained from the dependence of the interfacial rate on [S*] are directly related to K_d, K_M* and k_{cat}* by eqs 3 (A9) and 4 (A10). The dissociation constant for E*, K_d, is independently measured using dispersions of a neutral diluent. K_M*, obtained from inhibition kinetics (eq A12b), and K_M^{app} provide values of K_M.

The effect of added NaCl on the observed rate is striking. It enhances the hydrolysis rate at zwitterionic micellar and vesicular interfaces without significantly affecting the rate of hydrolysis of monodispersed phospholipid or anionic vesicles and micelles. NaCl promotes binding of PLA2 to zwitterionic interfaces, which accounts for the salt-dependent decrease in K_M^{app}. Added NaCl increases V_M^{app} for zwitterionic substrates. In 4 M NaCl V_M^{app} values are comparable to those for hydrolysis of anionic phospholipid of the same chain length. Chemical trapping experiments show that the concentration of Cl^- at zwitterionic interfaces is proportional to the bulk Cl^- concentration. The independent electrophoretic mobility data of Tatulian (1983) show preferential binding of anions over cations to zwitterionic interfaces, imparting a net negative charge on the zwitterionic interface. Comparison of results with vesicles of long-chain zwitterionic phospholipid shows that the primary catalytic parameters do not significantly depend on the micellar or bilayer organization, although modest effects due to chain length are noted (Table 5). Collectively, these results show that the anionic charge at the interface is the key, if not the only, parameter influenced by the "quality of the interface".

Results in the last part show that added NaCl has little effect on the affinity of the bound enzyme for mimics (K_I*). The NaCl-induced increase in the binding of substrate mimics to the enzyme in the aqueous phase (K_I) is comparable to the effect on the cmc of the mimic (K_I'), suggesting that both processes are driven primarily by the hydrophobic effect. Similarly, added NaCl increases the binding of free enzyme to the interface (K_d) by the same factor as the binding of the enzyme−mimic complex to the interface (K_d^I). In short, analysis of the equilibria involved in the boxed region of Scheme 1 (eq A4) shows that the interface enhances binding of substrate mimics to the active site of E* (K_S* allostery) and that anionic charge at the interface enhances the E to E* step. Analysis of apparent rate parameters, K_M^{app} and V_M^{app}, in terms of the primary interfacial rate and equilibrium constants (eqs A5−A13) shows that the anionic charge at the interface enhances the E to E* step and the chemical step (k_{cat}* allostery). Thus, NaCl-induced decrease in K_M^{app} is due to a decrease in K_d, and the increase in V_M^{app} is due to an increase in k_{cat}* induced by an anionic character imparted to the interface by selective partitioning of Cl^- over that of Na^+.

MATERIALS AND METHODS

Sources of reagents and most experimental protocols are as described (Jain et al., 1986a−c, 1991a, 1995; Rogers et al., 1992, 1996). Only specific conditions for the present study are described below. DC_nPCs and the corresponding ethers (custom synthesis) were from Avanti Polar Lipids. MJ33 (Jain et al., 1991b), DC_nPM (Jain and Rogers, 1989) and $DC_{14}PC$-ether (Jain et al., 1986c) were synthesized previously. Preparation and characterization of 4-hexadecyl-

Table 1: Apparent Kinetic Parameters for the Hydrolysis of DC_nPC Dispersions in 10 mM $CaCl_2$ at pH 8.0 and 25 °C with Pig Pancreatic PLA2

conditions	K_M^{app} (mM) (K_S')[a] (mM)	K_d (mM)	K_M[d] (mM)	$X_I(50)$ (mol fraction)	K_M*[e] (mole fraction)	V_M^{app} (s^{-1})	V^{mono} (s^{-1})
DC_6PC + 0.001 M NaCl	>10	20				5.5	1.5
+ 0.1 M NaCl	7 (16)	20	0.6	0.015	0.10	10	1
+ 4 M NaCl	0.85 (1.4)	3.5	1.3	0.012	0.13	265	2.5
DC_7PC + 0.001 M NaCl	2.3 (1.5)	9.6	0.6	0.02	0.07	16	10
+ 0.1 M NaCl	2.0 (1.6)	7	0.31	0.03	0.05	28	8
+ 2 M NaCl	0.74 (0.35)	3.5	0.16	0.02	0.07	170	10
+ 4 M NaCl	0.2 (0.1)	1.3	0.3	0.012	0.13	660	*b*
DC_8PC + 0.001 M NaCl	1.44 (0.2)	10	0.06	0.04	0.035	250	30
+ 0.1 M NaCl	0.7 (0.14)	6	0.07	0.035	0.04	400	30
+ 2 M NaCl	0.27	2.8		0.02	0.07	1210	*b*
+ 4 M NaCl	0.06	0.95		0.02	0.07	2200	*b*
$DC_{14}PC$ + 0.001 M NaCl	*c*	4				73	*b*
+ 0.1 M NaCl	*c*	3				170	*b*
+ 1 M NaCl	*c*	1.4				220	*b*
+ 4 M NaCl	0.2	0.6		0.004	0.54	300	*b*
DC_8PM + 0.1 M NaCl	0.16	0.1		0.09	0.015	1260	*b*
+ 4 M NaCl	0.18					900	*b*

[a] cmc values are those measured at the salt concentration in column 1, and these values are subtracted from the phospholipid concentrations to calculate K_M^{app} values obtained from results of the type shown in Figure 4. [b] cmc is too small to measure. [c] No meaningful value obtained for zwitterionic vesicles. However, on the basis of the product-induced charge effects considered under Discussion, K_M^{app} values should decrease with increasing mol fraction of the products of hydrolysis (Jain & Jahagirdar, 1985). V^{mono} values were obtained from *y*-intercepts of plots of type shown in Figure 4 (eq 2). [d] K_M values in column 4 were obtained with eqs A10 and A14 from K_M^{app} and K_M* (column 6). [e] K_M* were obtained from $X_I(50)$ for MJ33 at saturating [S*].

2,6-dimethylbenzenediazonium tetrafluoroborate (16-ArN_2BF_4) and the reaction products, 16-ArOH, 16-ArH, and 16-ArCl, are described elsewhere (Chaudhuri et al., 1993). RM3 was kindly provided by Dr. Ronald Magolda (DuPont Co., Wilmington, DE). Mono- and dithiolesters of phosphatidylcholines were kindly provided by Dr. Stewart Hendrickson (University of Washington, Seattle). All other reagents were of analytical grade. Protocols used in this study are based on methods established in our laboratory (Jain et al., 1995), and only salient details are described below. All studies were carried out with pig pancreatic PLA2. Uncertainty in measured rates is 10%, and that in derived parameters is 30%.

Kinetic Protocols. Unless stated otherwise, kinetic measurements were carried out in polypropylene cups containing aqueous 10 mM $CaCl_2$ and 1 mM NaCl at 25 °C and pH 8.0 under a stream of nitrogen according to the pH-stat method using a Brinkman (Metrohm) or a Radiometer titrator with 3 mM NaOH as the titrant (Jain et al., 1986a; Jain & Gelb, 1991). Reaction progress was recorded on a strip chart recorder. Stock dispersions of DC_nPC in water were added to the reaction mixture and equilibrated. The background pH drift was negligible (<2%) compared to the observed rates. Reaction was initiated by the addition of PLA2 (0.1−30 pmol); the amount used varied depending on the observed rate. Hydrolysis commenced in <3 s after addition of enzyme, and the observed rate varied linearly with enzyme concentration. When inhibitor or other components were needed in the reaction mixture, they were added before the enzyme. Results reported here have been corrected for a small change in titration efficiency for released fatty acid in the presence of added NaCl, determined by adding a known amount of myristic acid or heptanoic acid to the reaction mixture in the absence of PLA2. Controls showed that the order of addition of substrate and PLA2 does not noticeably affect the values of K_M^{app} and V_M^{app}. Initial rates are expressed as turnover number per second.

Table 2: Measured and Normalized Yields of 16-ArOH and 16-ArCl and Interfacial Cl^- Concentration, $Cl_m^•$, Obtained from Dediazoniation of 0.22 mM 16-ArN_2^+ in Aqueous Dispersions of Phospholipid at 25 °C

		normalized yields		
phospholipid	[NaCl] (M)	% 16-ArOH	% 16-ArCl	$[Cl_m]$ (M)
DC_8PC (1.68 mM)	0	100	0.62	
	0[a]	100	0.46	
	1[a]	89.31	10.7	0.9
	2[a]	79.8	20.2	2.0
$DC_{14}PC$ (1.0 mM)	0[b]	100	0.8	
	1.14[b]	93.9	6.1	0.4
	2.0[b]	88.7	11.3	0.9
	0	100	0.8	
	1.15	93.8	6.2	0.4
	2.0	88.7	11.3	1.0
POPC	0[b]	100	0.7	
	1.14[b]	93.1	6.9	0.5
	2.0[b]	87.1	12.9	1.1

[a] Solutions contain 10 mM HCl. [b] Solutions contain 0.1 mM HCl.

Determination of the cmc. Values of the cmc (= K_I' or K_S') listed in Tables 1 and 3 were determined by surface tension using a Roller-Smith surface tension balance (Du Nouy ring design) in 4 mL of 10 mM Tris buffer at pH 8.0 and 25 °C containing other salts at indicated concentrations. Solutions were stirred after addition of each aliquot of phospholipid dispersion.

Estimating Chloride Ion Concentration at Interfaces. Concentrations of Cl^- at zwitterionic interface of DC_nPC micelles or vesicles (Table 2) were estimated by the chemical trapping method (Chaudhuri et al., 1993; Cuccovia et al., 1997). The chemical probe 4-hexadecyl-2,6-dimethylbenzenediazonium ion (16-ArN_2^+) binds to phospholipid aggregates and covalently reacts with weakly basic nucleophiles (Cl^- and water) at the aggregate interface. The long hydrocarbon chain ensures complete partitioning of 16-ArN_2^+ into the aggregates, and its cationic charge ensures that the reactive diazonio group is oriented at the aggregate interface. Yields of 16-ArCl are proportional to the concentration of

Table 3: [NaCl] Dependence of K_I' and K_I Values[a] (Millimolar) for Zwitterionic Substrate Mimics of PLA2

mimic (= I)	K_I' at NaCl = 0.1 M	K_I' at NaCl = 4 M	K_I at NaCl = 0.1 M	K_I at NaCl = 4 M	K_I* at NaCl = 0.1 M	K_I'/K_I at NaCl = 0.1 M	$K_I/K_I'K_I$* at NaCl = 0.1 M
DC_6PC-ether	5.3	0.4	1	0.089	0.4	5.3	0.5
DC_7PC-ether	0.3	0.02	0.08	0.0026	0.2	3.8	1.3
MJ72	0.3		0.086		0.0005	170	12
MJ33	0.01		0.008		0.0014	25	29
RM3	4(1)		0.07		0.0004	120	21
MG14	1		0.04		0.00014	70	102

[a] The K_I values were obtained by the protection method (Jain et al., 1993b). K_I' values are the cmc values. New (K_I') value for RM3, K_I*, and the K_I'/K_I ratio for the inhibitors are estimates from results of type shown in Figure 9B (eqs A12a and A13b). Activation factor $K_I/K_I'K_I$* was calculated from the K_I* and the K_I'/K_I ratios fom the kinetic method.

Table 4: Dissociation Constants[a] K_d (Millimolar), K_d(I) (Millimolar), and K_I* (Mole Fraction) for Pig PLA2

	1 mM NaCl					4 M NaCl		
mimic (= I)	K_d	K_d(I)	K_I*	K_d^I	K_d/K_d^I	K_d	K_d(I)	K_I*
DC_6PC-ether			0.4					0.35
DC_7PC-ether	9.6	2.4	0.2	1.5	6.4	1.1	0.15	0.2
DC_8PC-ether	10	2.3	0.1	2.5	4	0.94	0.16	0.15
DC_{14}PC-ether	8	3.6	0.5	6.6	13	0.3	0.15	0.5
deoxy-LPC	3.7	2.8	>2			0.3	0.2	>2
+ MJ72[b]	0.9		0.0027	0.028	32			
+ MJ33[b]	0.9		0.0014	0.02	45			0.002
+ RM3[b]	0.9		0.0033	0.15	6			0.005
+ MG14[b]	0.9		0.0009	0.028	32			

[a] Uncertainty in these results is ±30%. The K_d and K_d(I) (at X_I = 1 mol fraction) for the ethers are measured by fluorescence method (Figure 8). K_I* values were obtained by the protection method. K_d^I values for ethers were calculated from K_d(I), K_I* and K_d (eq 1). [b] Values from Jain et al. (1993b). The new K_d value (= 3.7 mM) for deoxy-LPC is about 4-fold larger than that reported earlier (= 0.9 mM). This could possibly be due to an inhibitory contamination in the earlier preparation of deoxy-LPC.

Cl^- in the interfacial region and to the selectivity of the dediazoniation reaction toward Cl^- versus H_2O, which is estimated from competition experiments in bulk aqueous tetramethylammonium chloride (TMACl) solution (see below).

Dediazoniation reactions in the presence of added NaCl were carried out in aqueous dispersions of DC_{14}PC, POPC, and DC_8PC at 25 °C. Reactions were initiated by adding an ice-cold, freshly prepared solution of 0.011 M 16-ArN_2-BF_4 in acetonitrile. Reactions were complete after 3 days (half-time ≈ 5 h at 25 °C), and 16-ArOH and 16-ArCl are major products. Yields of individual products were determined by using a Perkin-Elmer HPLC system composed of a Series 410 quaternary pump, an ISS 200LC autosampler fitted with a 20 μL loop, an LC-235 diode array detector, and a PE-Nelson 900 Series interface attached to an Ultra PC computer for data analysis using Turbochrom 3 software. Products were separated on a Rainin C_{18} reversed-phase column (5 μm, 4.6 mm i.d. × 25 cm) using a mobile phase of 64% methanol and 36% 2-propanol with flow rates of 0.8 mL/min and monitored at 220 nm. Typical retention times for the major products were 7.5 min for 16-ArOH and 18 min for 16-ArCl. The phospholipid eluted in <5 min. Product identities were confirmed by spiking runs with independently synthesized standards. Yields of 16-ArOH and 16-ArCl in the product mixtures were estimated from average peak areas (two or three injections) by using calibration curves prepared with standards. Interfacial Cl^- concentrations, $[Cl_m]$, in units of moles per liter of the reaction volume, were estimated from %16−ArCl yields by assuming that the selectivity of the dediazoniation reaction toward Cl^- and H_2O at aggregate interfaces is the same as that of water-soluble short-chain analogue 1-Ar^+ toward Cl^- and H_2O in aqueous TMACl solutions. We assume that 16-ArCl yield from reaction with $[Cl_m]$ in the aggregates is the same as the 1-ArCl yield from reaction with Cl^- in an equivalent [TMACl] in aqueous solutions.

Total yields of 16-ArOH + 16-ArCl varied between 60 and 80% with two runs outside this range at 36 and 83%. These variations are caused by uncertainties in the weight of the arenediazonium salt used to prepare its stock solution (∼5 mg) and possible reaction of the arenediazonium ion with the phosphate group of the phospholipid, although no additional products were observed in the chromatogram. Either these acylphosphate ester products hydrolyzed rapidly to 16-ArOH and phospholipid, or they have short retention times, i.e. <5 min, and are in the void volume peaks. Our primary focus is on the changes in $[Cl_m]$ with added NaCl, and we report the relative (normalized) yields of the two major products, 16-ArOH and 16-ArCl only for comparative purposes. Two minor products, 3,5-dimethylhexadecylbenzene and *N*-4-hexadecyl-2,6-dimethylphenylacetamide, are formed by reaction of 16-ArN_2^+ with 16-ArOH and acetonitrile and they elute at 5 and 14 min, respectively. These products are formed competitively with 16-ArOH and 16-ArCl but in such small amounts that they do not affect the estimated yields of 16-ArOH and 16-ArCl significantly (Romsted & Yao, 1996).

Protection Method To Determine Binding of Active-Site-Directed Mimics to PLA2. As detailed elsewhere (Jain et al., 1991a; Yu et al., 1993), the time course of inactivation of PLA2 by PNBr, which modifies the catalytic His-48, provides a measure of the occupancy of the active site and permits determination of the equilibrium dissociation constants for the binding of mimics to E or E*, defined as K_I or K_I* (Tables 3 and 4). The 0.03 mL alkylation reaction mixture in a 6 × 50 mm borosilicate glass tube consisted of 0.1−1 μM PLA2 in 50 mM cacodylate buffer at pH 7.3, 0.1

M NaCl, 0.5 mM $CaCl_2$, 0.03 mg of γ-globulin, 2 mM PNBr, and an appropriate amount of a mimic at 23 °C. In cases when the dissociation constant at the interface is being measured (Table 4), the incubation mixture also contained 1.65 mM deoxy-LPC as the neutral diluent, which provides a micellar interface for the binding of PLA2, but individual deoxy-LPC molecules do not bind to the active site of the bound enzyme (Jain et al., 1991a,b). At various time intervals, an aliquot of the incubation mixture containing 0.01−10 pmol of enzyme was added to 1.5 mL of fluorescent lipid assay solution containing 1 μg of 1-palmitoyl-2−pyrenedecanoylglycero-3-phosphomethanol (Molecular Probes), 250 μg of BSA (Sigma), 0.1 M NaCl, 0.25 mM $CaCl_2$, and 50 mM Tris buffer at pH 8.5 and 23 °C (Yu et al., 1993, 1997; Bayburt et al., 1995). The assay solution was pre-equilibrated for 2−3 min to stabilize the baseline before addition of the aliquot from the alkylation solutions. Residual activity was detected as an increase in the fluorescence at 396 nm (excitation at 345 nm on an SLM 4800S spectrofluorometer) at each time interval.

Measurement of K_d (E to E) and K_d^I (E*I to EI).* The dissociation constant, K_d, was calculated from the binding isotherms obtained by monitoring the change in the fluorescence emission from Trp-3 at 333 nm from PLA2 as a function of bulk deoxy-LPC concentration (Jain et al., 1993b). K_d^I values were obtained by titration of EI, in a mixture of PLA2 and saturating amounts of the mimic, with deoxy-LPC. K_d values were also obtained from the titration curve for the addition of dispersions of DC_nPC-ether to PLA2 in the absence of calcium (Tables 1 and 4). The $K_d(I)$ values for ethers in Table 4 were obtained from the titration curves (Figure 8) in the presence of calcium because calcium-dependent binding of a substrate mimic shifts the equilibrium in favor of the E*I form. Consider two equilibria from the boxed region of Scheme 1:

Scheme 2

$$\text{E (+ neutral diluent)} \rightleftarrows \text{E}^* + \text{I}^* \rightleftarrows \text{E}^*\text{I} \rightleftarrows \text{EI (+ neutral diluent)}$$

$$K_d(\text{I}) = \frac{[\text{ND}]([\text{E}] + [\text{EI}])}{[\text{E}^*] + [\text{E}^*\text{I}]} = \frac{K_d K_I^* + X_I K_d^I}{X_I + K_I^*} \qquad (1)$$

Thus, $K_d(I)$ describes the composite dissociation constant for E*I and E* to EI and E. $K_d(I)$ equals K_d in the limit when I does not bind the catalytic site, $K_I^* \gg 1$, and equals K_d^I when $K_I^* \ll X_I$. Results with several mimics show that the binding of the mimic to the active site of PLA2 requires calcium as an obligatory cofactor but that the binding of PLA2 to the interface does not (Yu et al., 1993). Thus, any lipid is a neutral diluent for PLA2 in the absence of calcium. The fluorescence signal for E* and E*I forms depends on the nature of the amphiphile. Values of K_d and $K_d(I)$ could not be measured for DC_6PC-ether, which gave a very small spectral signal.

Chromatographic Protocols for Interfacial Binding: E to E and EI to E*I.* The binding of PLA2 to phospholipid dispersions was monitored according to previously established spectroscopic methods based on the change in the emission from Trp-3 (Jain et al., 1982, 1986b, 1993b) or by the fluorescence resonance energy transfer signal from a dansyl probe in the interface (Jain & Vaz, 1987). In addition, a HPLC protocol using an IAM.PC.DD column (Model 777007, serial no. 10075 and 10098 from RegisTechnologies, Morton Grove, IL) provided an independent, rapid, and sensitive measure of K_d and K_d^I. The IAM stationary phase consists of silica beads with a close-packed monolayer of decylphosphocholine immobilized by covalent linking via the methyl terminus of the alkyl chain (Ong et al., 1996; Pidgeon & Venktarum, 1989). Elution profiles were monitored at a flow rate of 0.5 mL/min in 10 mM Tris at pH 8.0 with Rainin HPLC hardware sequentially equipped with absorbance and fluorescence detectors. The interface of the immobilized monolayer is assumed to resemble that of phosphatidylcholine vesicles or micelles, except that individual amphiphiles cannot be perturbed or dislodged, and thus the matrix amphiphile cannot enter the active site of PLA2. Reciprocal of the retention time ($1/t_r$) is proportional to the K_d, and thus relative changes are correlated. In the presence of a saturating amount of an inhibitor at the interface, $1/t_r$ is related to K_d^I. We have obtained comparable results with several different IAM columns. However, in our experience the stability of IAM columns is erratic and the imidazole capping material sometimes eluted during a gradient (typically after 1 L of flow through) and the column becomes useless as it develops a net negative charge.

RESULTS

Key Considerations for the Analysis of Interfacial Catalysis in Micellar Solutions. According to Scheme 1, the observed rate is the sum of the catalytic turnover by two paths. The magnitudes of the primary rate and equilibrium parameters for the catalytic turnover via E*S (k_{cat}* and K_M*) and ES (k_{cat} and K_M) complexes determine the intrinsic catalytic efficiency of PLA2 in the micellar and aqueous phases, respectively. Quantitative interpretation of this model is based on two conditions, fundamental to any kinetic analysis but they assume special significance for Scheme 1. (a) The detailed balance condition is a thermodynamic statement of the relationship between the component equilibria (Jain et al., 1993b). (b) The microscopic steady-state condition requires that at any given time during the reaction progress each enzyme molecule in the reaction mixture experiences the same average microscopic environment and that the catalytic turnover remains rate limiting (Berg et al., 1991). A complete analysis of PLA2-catalyzed turnover on short-chain phosphatidylcholine micelles in terms of the primary rate and equilibrium parameters (eqs A5 and A6) is possible within the following experimentally verifiable assumptions:

(i) Below the cmc the solutions contain monodisperse substrate amphiphile. Above the cmc, excess substrate molecules form micelles and exchange rapidly with monodisperse phospholipid molecules in the aqueous phase. Thus, the bulk concentration of phospholipid present as micelles, [S*], equals [S_{tot}] − cmc; here and elsewhere square brackets indicate bulk concentrations in moles per liter of aqueous solution volume.

(ii) The fraction of the total enzyme at an interface increases with [S*]. The dissociation constant is defined as K_d for the E* form and as K_d^I for the E*I form.

(iii) The amount of substrate available for the hydrolysis increases with increasing [S*]; however, X_S, the substrate concentration at the interface expressed in mole fraction units, within micelles that the bound enzyme "sees" is independent

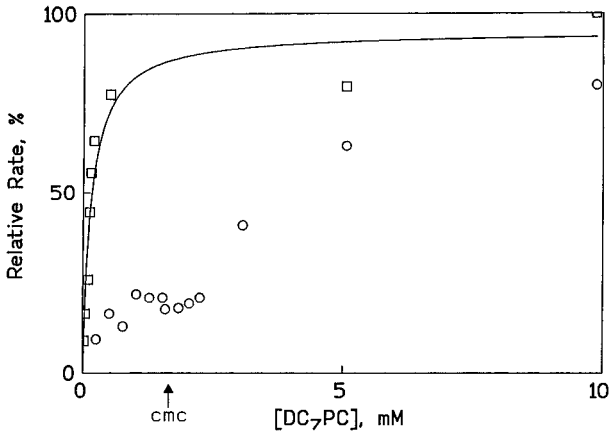

FIGURE 1: Relative rates (with 100% for respective V_M^{app}) of hydrolysis as a function of DC_7PC concentration in (circles) 0.1 M or (squares) 4 M NaCl by (0.05−1 μg) pig pancreatic PLA2 determined by pH-stat titration at pH 8.0 and 24 °C in 10 mM $CaCl_2$. The maximum rate at both salt concentrations corresponds to V_M^{app} values listed in Table 1. The arrow marks the cmc in 0.1 M NaCl. As shown in Figure 4, V_M^{app} values were obtained from the rate with micellar substrate (eq 2).

of [S*]. In the absence of additive, $X_S = 1$ (unity) at the start of the reaction.

(iv) When the aggregate size is small compared to the turnover rate, the "initial substrate concentration" that bound enzyme "sees" at the interface changes rapidly during the course of the reaction, unless of course the substrate replenishment and the removal of the products are faster than the rate of catalytic turnover.

Hydrolysis of Short-Chain Phosphatidylcholines. Reaction progress for the hydrolysis of the aqueous solutions of DC_nPC ($n = 6-8$) by PLA2 has been extensively studied (de Haas et al., 1971; Pieterson et al., 1974; Jain & Rogers, 1989). Reaction begins immediately after addition of enzyme. Initial rates are linear, but they decrease gradually until all of the substrate is consumed. Intrinsic enzyme activity remains undiminished because hydrolysis begins again when a fresh aliquot of DC_nPC is added to the reaction mixture. The relationship between the initial rate of hydrolysis and [DC_7PC] is complex (Figure 1, circles). Below the cmc (1.5 mM for DC_7PC in 1 mM or 0.1 M NaCl), the initial rates of hydrolysis increase with DC_7PC concentration, and the absolute values of these rates are consistent with earlier results (de Haas et al., 1971; Pieterson et al., 1974; Verheij et al., 1981). We have reported estimates of the Michaelis parameters for the hydrolysis of DC_nPCs via the ES branch (Rogers et al., 1992). These are in accord with values of V^{mono} and K_M (Table 1) determined independently as described below.

NaCl Increases the Rate above the cmc. The observed rate above the cmc is the sum of the hydrolysis rates of monodisperse and micellar substrate. The contribution of the rate of hydrolysis of monodisperse substrate decreases as [S*] increases and more enzyme binds to micelles. As shown in Figure 1, the normalized initial rate of hydrolysis of DC_7PC increases above the cmc and approaches a plateau in 0.1 and 4 M NaCl. At higher [NaCl] the observed rate increases more rapidly at much lower substrate concentrations, in part because of a NaCl-induced decrease in the cmc (next section). The actual value of the maximum rate in 4 M NaCl is >30-fold higher than in 0.1 M NaCl. Similar NaCl-induced increases in the rate were observed for all

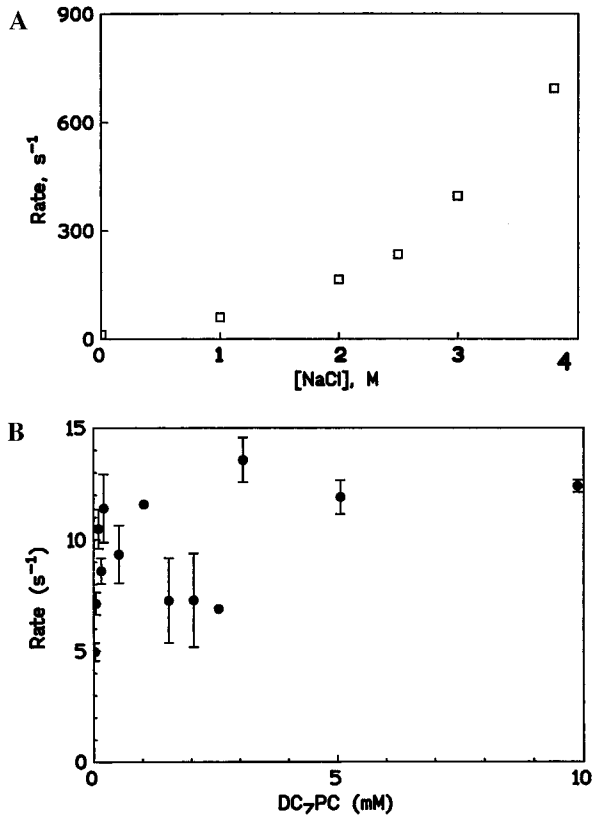

FIGURE 2: (A) Effect of added NaCl on the rate of hydrolysis of 10.4 mM DC_7PC by PLA2 in 10 mM $CaCl_2$; (B) dependence of the rate of hydrolysis at 10 mM $CaCl_2$ and 1 mM NaCl by PLA2 as a function of bulk DC_7PC concentration. Both sets were obtained with 0.1−1 of μg PLA2 at pH 8 and 25 °C.

homologous phosphatidylcholines. The apparent rate of hydrolysis of DC_7PC micelles increases with NaCl concentration (Figure 2A). Note that even at the maximum NaCl concentration (its solubility limit) the observed rate does not saturate. As shown in Figure 2B, an increase in the observed rate above the cmc is insignificant in 1 mM NaCl; that is, in the absence of added NaCl, the rate of hydrolysis of micellar substrate by PLA2 is virtually the same as that of the monodisperse substrate.

In short, the observed increase in the rate above the cmc is almost entirely due to the presence of added NaCl. This phenomenon is characterized first in terms of the apparent parameters (eq A6 parametrized as eq 2), that are analyzed later to obtain primary rate and equilibrium constants. The effect of NaCl on the observed rate of hydrolysis of zwitterionic phospholipid dispersions was analyzed in terms of the effect on individual equilibrium constants in Scheme 1. The analysis developed below shows that two phenomena are critical for understanding the effect of added NaCl on the observed kinetics: selective partitioning of ions at interfaces (Collins & Washabaugh, 1985; Tatulian, 1983; also see below) and salting out of nonpolar solutes (Mukerjee, 1965).

NaCl Lowers the cmc (K_I' and K_S'). Salting out of monomer amphiphiles from the aqueous phase to an aggregate lowers the distribution constant of an amphiphile. We use K_S' to denote the distribution constant of substrate and K_I' for the mimic, which by definition are equal to the cmc (eqs A1 and A2). Like dissociation constants, its inverse reflects the tendency of an amphiphile to partition into its own interface; however, it must also relate to the partitioning

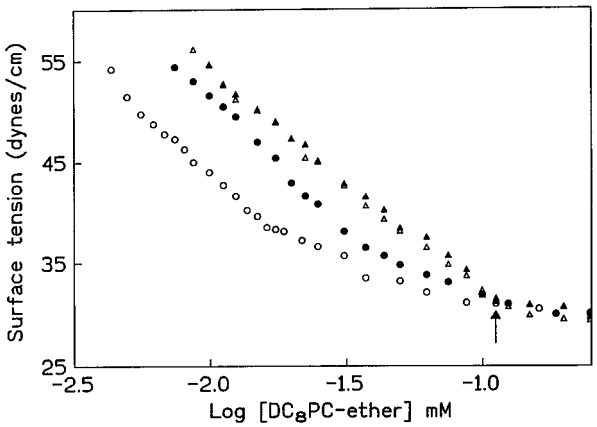

FIGURE 3: Change in the surface tension of (triangles) 0.1 M NaCl or (circles) 4 M NaCl in 10 mM Tris at pH 8.0 on the addition of DC_8PC-ether (on the log scale) (open symbols) without or (solid symbols) with 3.88 μM pig PLA2. Stock solutions of the ether were kept in ethanol, and the ethanol concentration in the bulk solution did not exceed 0.5%.

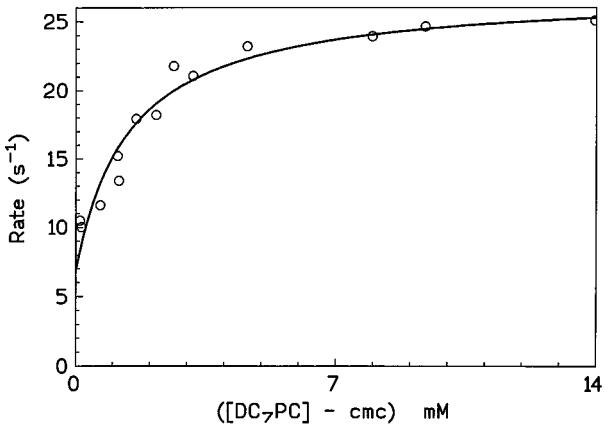

FIGURE 4: Dependence of the rate of hydrolysis by (0.1−1 μg) pig PLA2 in 0.1 M NaCl as a function of aggregated [DC_7PC]. Values of V^{mono}, K_M^{app}, and V_M^{app} were obtained by fitting (solid curve) data to eq 2.

tendency in other lipid/water interfaces. As shown in Figure 3, the surface tension of 0.1 M aqueous NaCl solution decreases on addition of DC_8PC-ether, and the break point, marked by an arrow, is defined as the cmc. The K_S' and K_I' values in Tables 1 and 3 were obtained by this method, and values for DC_nPC are consistent with the published values (Tausk et al., 1974a−c; Lin et al., 1990). Plots of log K_I' of DC_nPC-ether as a function of [NaCl] are generally linear up to 4 M NaCl, and the slope depends on the chain length (not shown). A variety of salts lower the cmc of DC_nPC (Tausk et al., 1974a−c) and other amphiphiles in aqueous solution, and log cmc vs [salt] plots are generally linear (Mukerjee, 1965; Fendler, 1982).

As also shown in Figure 3, addition of PLA2 produces a marked increase in the surface tension in 4 M but not in 0.1 M NaCl. At low lipid concentrations used in these experiments, the lipid is not in large excess over PLA2. For example, at log [DC_8PC-ether] = −2 (or 10 μM), the lipid/PLA2 mole ratio is ∼3. No clear break point is observed in 4 M NaCl in the absence or presence of 3.66 μM PLA2, and the cmc is indeterminate. The absence of a sharp clear transition in 4 M NaCl suggests that aggregate formation is not highly cooperative but may be stepwise. If so, the approximation of the pseudophase model for micelles does not hold. In short, added PLA2 increases the surface tension in 4 M, but not in 0.1 M, NaCl suggesting salt-induced formation of PLA2+DC_8PC-ether complexes (in the bulk aqueous phase) that are less surface active than DC_8PC-ether alone.

NaCl Changes the Apparent Kinetic Parameters, K_M^{app} and V_M^{app}, for the Hydrolysis of DC_nPC Micelles. Initial hydrolysis rates at higher [NaCl] show a hyperbolic dependence on DC_nPC (n = 6−8) concentration in the micellar form, [S*]. Expressed in terms of apparent parameters, eq A6 reduces to eq 2. As plotted in Figure 4 for DC_7PC in 0.1 M NaCl, the nonlinear regression fit to eq 2 is reasonable (r^2 >0.98 with <30% standard deviation). K_M^{app} and V_M^{app} values change with the substrate chain length and [NaCl] (Table 1). In 4 M NaCl, the maximum rate of hydrolysis of DC_8PC and the apparent affinity of PLA2 for the interface are comparable to those for the hydrolysis of micellar anionic DC_8PM in the absence of salt. Note that the rate of hydrolysis of DC_8PM decreases modestly in 4 M NaCl [Table 1; see also Jain and Rogers (1989) and Rogers et al. (1996)], suggesting NaCl-induced displacement of PLA2 from the anionic aggregates (see Discussion). V^{mono} values, obtained as the y-intercept at [S*] = 0 (Table 1, last column), are generally within a factor of 2 of the maximum initial rates measured at [DC_7PC] below the cmc (Rogers et al., 1992).

$$v_0^0 = \frac{V_M^{app}[S^*] + V^{mono}K_M^{app}}{[S^*] + K_M^{app}} \qquad (2)$$

NaCl Promotes the Hydrolysis of Zwitterionic Vesicles by PLA2. Apparent activating effects of NaCl on the hydrolysis of $DC_{14}PC$ and POPC vesicles are shown in Figure 5. Lag periods are observed during the hydrolysis of $DC_{14}PC$ vesicles at low salt concentration because of weak binding of PLA2 (Upreti & Jain, 1980; Apitz-Castro et al., 1982). An abrupt increase in the rate is seen only after sufficient anionic amphiphilic product is generated in the vesicles to promote PLA2 binding to vesicles (Jain et al., 1982). Thus, the lag period represents the time required for the formation of a critical mole fraction of anionic hydrolysis product at the interface, and the steady-state rate after the lag period reflects enhanced rate due to an increasing fraction of the enzyme at the vesicle interface (Jain & Berg, 1989).

A critical anionic charge density at the interface is required for the PLA2 binding, and local distribution of the charged amphiphiles is determined by the phase properties (Jain et al., 1989). This is best illustrated by results in Figure 5. The phase separation of the products occurs at lowest mole fraction near the gel−fluid transition of $DC_{14}PC$ at 24 °C and is not favored in the fluid bilayers of POPC (Jain & Berg, 1989; Jain et al., 1989). The results in Figure 5A show that added NaCl shortens the lag period and no lag is observable in 4 M NaCl. The steady-state rate observed at the end of the lag period in Figure 5A, 160 s^{-1}, is comparable to the initial rate of 210 s^{-1} observed in 4 M NaCl and 170 s^{-1} observed with ternary covesicles of $DC_{14}PC$ with 10 mol % hydrolysis products [see Apitz-Castro et al. (1982)]. These modest differences in rate are consistent with small differences in X_S and product inhibition.

Added NaCl affects the hydrolysis of POPC vesicles (Figure 5B) which show gel−fluid transition below 10 °C. At low [NaCl], the rate of hydrolysis is barely above the background level, but it increases significantly at higher NaCl

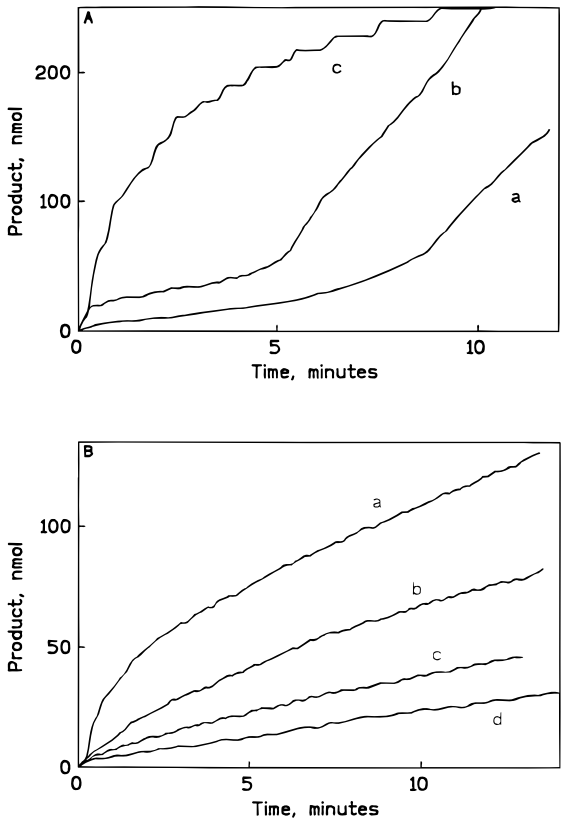

FIGURE 5: (A) Reaction progress curves for the hydrolysis of $DC_{14}PC$ vesicles in the presence of 9.35 pmol of PLA2 at pH 8.0 and 25 °C in 4 mL of 10 mM $CaCl_2$ and (a) 1 mM, (b) 0.2 M, and (c) 4 M NaCl in the reaction medium; (B) reaction progress for 0.32 mM POPC vesicles in the presence of 9.35 pmol of pig PLA2 at pH 8.0 and 25 °C in 4 mL of 10 mM $CaCl_2$ and (a) 4 M, (b) 1 M, (c) 0.5 M, and (d) 0.2 M NaCl.

concentrations. These results parallel the effect on the observed rate of PLA2-catalyzed hydrolysis of POPC covesicles containing an increasing mole fraction of anionic phospholipid (Ghomashchi et al., 1991). Note that a lag period is not seen with POPC vesicles because the products of hydrolysis mix ideally within the fluid phase bilayers, and thus sufficient local anionic charge density does not develop during the reaction progress.

Selective Partitioning of Chloride Ion into Zwitterionic Interfaces. A chemical trapping method was used to estimate interfacial chloride concentrations [Cl_m] in DC_nPC micelles and vesicles. Product yields from reaction of aggregate bound 16-ArN_2^+ have been shown to provide reasonable estimates of interfacial concentrations of weakly basic nucleophiles such as halide ions and alcohols in cationic micelles (Chaudhuri et al., 1993; Romsted & Yao, 1996; Cuccovia et al., 1997).

Formation of 16-ArCl from dediazoniation reactions in phospholipid dispersions provides direct evidence for the partitioning of Cl^- into the zwitterionic interfaces. Table 2 lists normalized yields of 16-ArOH and 16-ArCl and estimates of [Cl_m] at interfaces of DC_8PC micelles and DMPC and POPC vesicles. Values of [Cl_m] estimated from these data are about the same as the bulk NaCl concentration, although these estimates are only approximate (see Materials and Methods). The crucial result is that the yield of 16-ArCl increases with added [NaCl] in micelles and vesicles. At comparable NaCl concentrations the yield of 16-ArCl in DC_8PC micelles is approximately twice that in DMPC or POPC vesicles. The near equivalence of the aqueous and micellar Cl^- concentrations indicates that the barrier to penetration of the interface by Cl^- is minimal but that it may be greater for the bilayer interface than for the micellar interface. In short, these results show that Cl^- partitions into zwitterionic interfaces. Development of a net negative charge, as a consequence of selective partitioning of anions, is clearly demonstrated by a change in the electrophoretic mobility of $DC_{14}PC$ multilamellar liposomes (Tatulian, 1983). Selective binding of anions over cations to zwitterionic interfaces is indicated by other measurements as well (Collins & Washabaugh, 1985; Bapista et al., 1992; Bunton et al., 1987, 1989, 1991; Correia et al., 1992; Fendler, 1982).

Modeling the Rate Enhancement at Zwitterionic Interfaces by Added NaCl. The results described so far show that added NaCl increases the micelle concentration by lowering the cmc and that a selective partitioning of Cl^- imparts a net negative charge to zwitterionic micelles and vesicles. Added NaCl lowers K_M^{app} and increases V_M^{app} for PLA2-catalyzed hydrolysis of zwitterionic micelles but does not influence the PLA2-catalyzed rate of hydrolysis of anionic phospholipid aggregates (Table 1). Equations 3 and 4 (eqs A9 and A10 in the Appendix) define the relationships between the apparent parameters and the primary rate and equilibrium constants. K_M and K_M* are the Michaelis constants for the hydrolysis via the ES and E*S complexes, respectively. The effect of NaCl on the individual equilibria that precede the chemical step are analyzed below.

$$V_M^{app} = k_{cat}^*/(1 + K^*_M) \quad (3)$$

$$K_M^{app} = \frac{K_d K_M^*}{1 + K_M^*}\left(1 + \frac{K_S'}{K_M}\right) \quad (4)$$

$$K_S' = K_d^S K_S / K_d K_S^* \quad (5)$$

$$K_I' = K_d^I K_I / K_d K_I^* \quad (6)$$

As shown earlier, there is a significant salt effect on K_S' for DC_nPC (Table 1). K_S' is related to four other equilibria of the thermodynamic cycle by detailed balance condition (eq 5). Due to catalytic turnover, the equilibria on the right side of eq 5 cannot be measured directly for a substrate on an interface. However, protocols developed earlier (Jain et al., 1993b) demonstrate that an equivalent relationship (eq 6) holds for several substrate mimics at low and high NaCl concentrations. The operating principle for the detailed balance condition is that when going round a full cycle of changes in the thermodynamic box, salt effects that appear in one branch must be fully compensated in some other branch(es), so that the overall free energy change is zero. Results in sequel show that the effect of added NaCl on K_I' is compensated by a change in K_I. Similarly, the effect of NaCl on K_d is compensated by an effect on K_d^I. There is no significant effect of added NaCl on K_I* or on K_M*.

Chemical Step Remains Rate Limiting with Added NaCl. In the scooting mode, the rate of hydrolysis of 1,2-dithiolester analogues of anionic $DC_{14}PM$ is about 10% of the rate of the corresponding dioxyesters (Jain et al., 1992). V_M^{app} for the dithiolester analogue of DC_8PC is also ~10% (results not shown) compared to the value for the DC_8PC (Table 1), and the element effect remains unchanged in 4 M NaCl. The

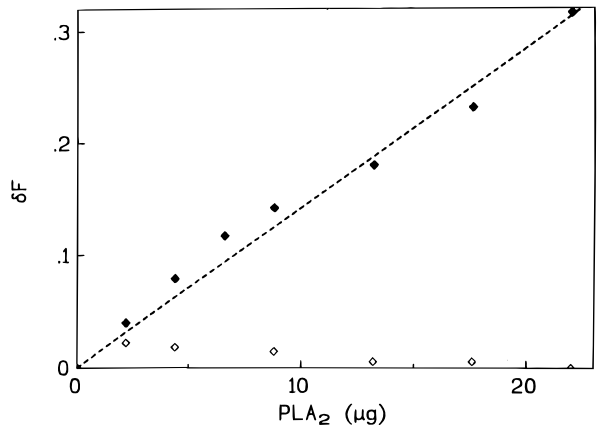

FIGURE 6: Increase in the resonance energy transfer emission intensity, δF, at 495 nm from Trp-3 of pig PLA2 added to covesicles of *N*-dansyl 1,2-ditetradecyl-*glycero*-3-phosphoethanolamine (2.5 mol %) and $DC_{14}PC$-ether in the presence of (open diamonds) 1 mM or (solid diamonds) 4 M NaCl in 10 mM Tris at pH 8.0 and 24 °C.

element effect is not seen in K_M^{app}. A 10-fold higher rate for the oxy analogue of the substrate suggests that the chemical step is fully rate limiting. If a physical change, such as diffusion or the rate of dissociation of E*P complex is rate limiting, an element effect of 10-fold is unlikely (Jain et al., 1993a). These results show that added NaCl or a change in the head group does not change the catalytic mechanism and the chemical step remains rate limiting at V_M^{app}, that is, substrate replenishment and product release from E*P are rapid on the time scale of the catalytic turnover on the enzyme-containing micelle.

NaCl-Induced Increase of the Mimic Binding to the Interface (K_I') and to E (K_I) Are of the Same Magnitude. K_S' for DC_nPC (Table 1) and K_I' for DC_nPC-ethers (Table 3) decrease with added NaCl. Added NaCl also reduces K_I for the dissociation of DC_nPC-ethers bound to PLA2 in the aqueous phase, and the magnitude of the decrease is comparable to that observed with K_I' for the same mimic. The magnitude of the salt effect depends on the structure of the mimic, and the effect is smaller for the short-chain analogues. This trend is consistent with our earlier observation that the binding of a mimic to PLA2 in aqueous phase is dominated by the hydrophobic effect (Jain et al., 1993b). Thus, the magnitude of the NaCl-induced change is as predicted by the salting-out effect (Mukerjee, 1965); that is, log K_I' or log K_I is proportional to [NaCl]. In short, a parallel NaCl dependence for K_I' and K_I shows that the hydrophobic effect dominates in both cases. These results suggest that added NaCl should have a similar effect on K_S.

Binding of PLA2 to the Interface Is Enhanced by [NaCl]. The K_d and K_d^I values obtained under different conditions are compared in Table 4. Three independent protocols showed that NaCl reduces the dissociation of E* (K_d) and E*I (K_d^I) from zwitterionic interfaces. The resonance energy transfer emission intensity from 2 mol % *N*-dansylditetradecylphosphatidylethanolamine in $DC_{14}PC$-ether vesicles increases with added PLA2 only in 4 M but not in 1 mM NaCl (Figure 6). Since PLA2 must come in close contact with the interface for the energy transfer (Jain & Vaz, 1987), these results show that the binding of PLA2 to zwitterionic interfaces is enhanced by added NaCl. Note that these effects are not due to a change in the organization of the lipid (Jain & Wu, 1977), nor does the high-affinity PLA2 binding to

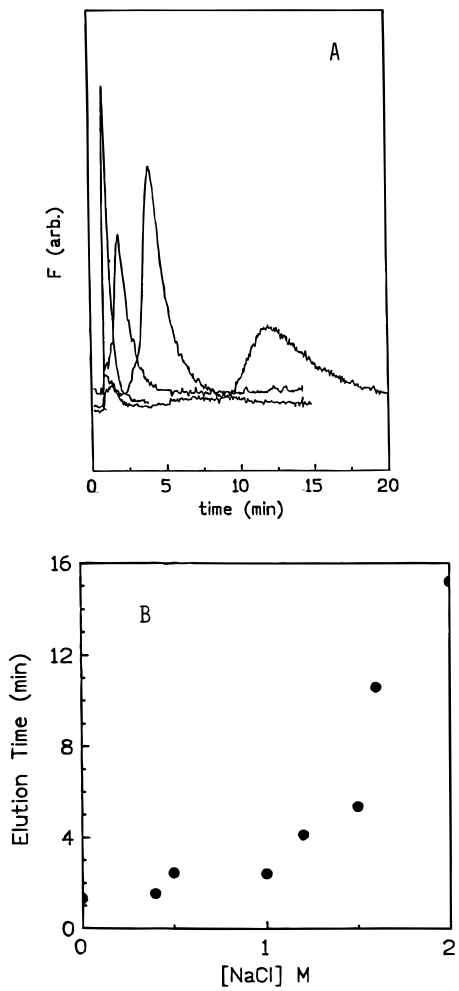

FIGURE 7: (A) Elution profiles for PLA2 from IAM-PC column with 10 mM Tris and 10 mM $CaCl_2$ (from left) with 0 M NaCl (peak at 1.37 min), 1 M NaCl (peak at 2.42 min), 0 M NaCl + 5 μM MJ33 (peak at 5.07 min) and 1 M NaCl + 5 μM MJ33 (peak at 14.9 min) (note that both the peak widths and elution times depend on the off-rate of the enzyme from the interface); (B) elution times as a function of [NaCl]. The flow rate for the HPLC runs was 0.5 mL/min, and the void volume time 0.97 min includes 0.3 min of the dead time for the flow through the HPLC flow system between the injector and the detector. Quantitative uncertainties in these results arise mostly from the fact that the retention time (t_r) at low salt is very close to the void volume (t_o).

anionic interfaces depend on the bilayer or micellar organization (Jain & Berg, 1989; Rogers et al., 1996).

For a quantitative comparison of the effect of [NaCl] on the dissociation of E* to E (K_d) and of E*I to EI (K_d^I), we adopted a chromatographic protocol that uses specific binding of PLA2 along its interfacial recognition region to a high-density immobilized monolayer of alkylphosphocholine (Ong et al., 1996). Here, retention times are quantitatively interpreted in terms of dissociation constants because the retention factor ($= t_r/t_0 - 1$) is proportional to the reciprocal of the dissociation constant. Added NaCl increases the retention time, t_r, of PLA2 from the IAM.PC column (Figure 7A). Also, the NaCl concentration dependence of t_r (Figure 7B) is comparable to that for NaCl-induced hydrolysis of DC_7PC (Figure 2A). The retention of PLA2 (related to K_d) and of its complex with MJ33 (related to K_d^I) is enhanced by NaCl to the same extent (Figure 7A); that is, the effects of added NaCl on K_d and K_d^I are comparable. For example, the increase in the retention time for E at 1 M NaCl is 3.6-fold (1.45/0.4) compared to a 3.4-fold (13.9/4.1) increase

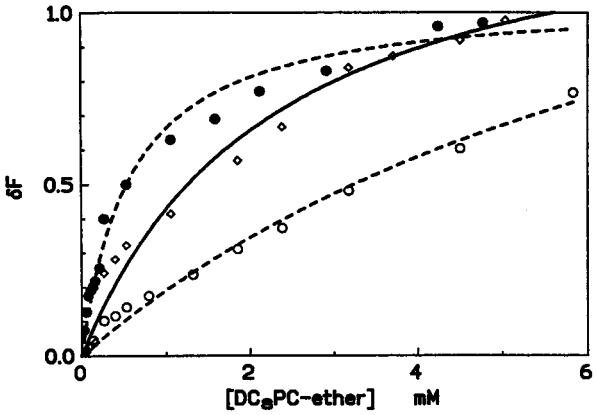

FIGURE 8: Increase in the fluorescence emission intensity, δF, at 333 nm (excitation at 280 nm with 4 nm slit widths) from Trp-3 of pig PLA2 as a function of DC_8PC-ether (bulk) concentration at (open circles) 1 mM NaCl and 0.2 mM EGTA, (solid circles) 4 M NaCl and 0.2 mM EGTA, or (open diamonds) 1 mM NaCl and 10 mM $CaCl_2$ in 10 mM Tris at pH 8.0 and 24 °C.

seen in the presence of MJ33. Note that retention of the PLA2·MJ33 complex is seen only in the presence of calcium, the obligatory cofactor for the binding of substrate mimics to the active site (Yu et al., 1993). The retention time of PLA2 alone does not change in the presence of calcium. Additional controls showed that the retention times on an IAM.PC column are related to the binding of PLA2 along the interfacial recognition region because pro-PLA2 is not retained. The seven extra residues at the N terminus of the zymogen are known to interfere with the binding to the interface (Verheij et al., 1981).

Independent measurement of K_d and K_d^I is also possible under certain conditions by monitoring the increase in the fluorescence emission intensity from Trp-3 of PLA2 as a function of bulk amphiphile concentration (Jain et al., 1982, 1993b; Jain & Maliwal, 1993). PLA2 binding isotherms in Figure 8 show several important features. The fluorescence intensity, δF, from Trp-3 of PLA2 increases with DC_8PC-ether concentration; however, the shape of the curves depends on the equilibria involved. K_d(I) values (Table 4), obtained from the data in the presence of calcium, contain information about several interfacial dissociation constants (Scheme 2). Estimates of K_d according to eq 1 are based on the equilibrium monitored as the change in the Trp emission intensity as a function of DC_8PC-ether concentration in the absence of calcium where the mimic does not bind the active site. The change in the fluorescence intensity as a function of the bulk concentration of DC_8PC-ether shows saturation behavior both in 1 mM and in 4 M NaCl. Fitting to a hyperbola gives the K_d values listed in Table 4. K_d in 1 mM NaCl is between 3 and 10 mM for the various phosphatidylcholine micelles and vesicles that we used as neutral diluents, and these values decrease 10−20-fold in the presence of 4 M NaCl.

Scheme 3

$$E\ (+\ \text{neutral diluent}) \rightleftarrows E^*$$

The titration curves in Figure 8 are useful for the determination of the dissociation constants only when the value is significantly >20 μM. This is because typically 1−5 μM PLA2 is required for these measurements and 20−50 amphiphiles bind to each PLA2. Thus, stoichiometric amount of lipid required for tight binding, ∼20−50 μM, would virtually completely mask the whole titration curve if the dissociation constant is significantly <20 μM. At 0.1 M NaCl, K_d^I values for E*I on deoxy-LPC micelles are in the 20−50 μM range (Jain et al., 1993b) and considerably lower on DC_{14}PM vesicles (Jain et al., 1986a; Berg et al., 1991). Therefore, this protocol provided only a qualitative indication that K_d^I is lower in the presence of added NaCl. Note that these upper limit estimates for K_d^I are also consistent with independently measured K_I* and K_d values (eq 1). In short, results in Table 4 show that the dissociation of E* and E*I forms decreases by 10-fold at 4 M NaCl.

$$\frac{X_I(50)}{1 - X_I(50)} = \frac{[S^*] + A}{[S^*]B + AC - K_S(1 + 2A/[S^*])} \quad (7)$$

Binding of Substrate Mimics to E (K_I*) Is Not Affected by Added NaCl.* The effect of NaCl on the binding of substrate mimics to the enzyme at the interface was evaluated by the protection method (Jain et al., 1991b; Yu et al., 1993). As summarized in Table 4, the effect of added NaCl on K_I* is modest. On the basis of eq 7 (parametrized from eq A12a), two limits are of interest in the dependence of $X_I(50)$ on [S*]:

(a) The [S*] dependence of the inhibition by MJ33, a competitive inhibitor, is shown in Figure 9A with A (= K_M^{app} in Table 1) and the fit parameters $B = 40$ and $C = 6$. With the cmc of 0.008 mM, MJ33 is virtually completely partitioned into the interface. At high [S*] the B term in the denominator dominates, and C dominates at low [S*]. The B-dominated relationship assumes the form (eq A12b) for the inhibition in the scooting mode (Berg et al., 1991); that $X_I(50)$ does not depend on [S*] for DC_8PC, as also shown for anionic DC_8PM micelles (Rogers et al., 1996) or DC_{14}PM vesicles (Jain et al., 1991a,b). These conditions provide a basis for the calculation of K_M* in Table 1, using K_I* = 0.0014 mol fraction.

(b) Results in Figure 9B show the dependence of $X_I(50)$ on [S*] for MJ72, a short-chain homologue with $K_I' = 0.3$ mM in deoxy-LPC (Jain et al., 1993b). The ordinate values are corrected according to eq A13b. The fitted curve gave $B = 106$ and $C = 42$. Since K_M* remains constant, the value of B (eq A12b) gives K_I* for MJ72 and other inhibitors (Table 3). These values are lower than the K_I* values on deoxy-LPC determined by the protection method (Table 4). Trends suggest it is unlikely to be scatter in the data. In addition to the arguments developed later, the K_I* values obtained by the protection and fluorescence methods give higher values because of the partitioning correction (Jain et al., 1993b).

Compared to MJ33, the value of C for MJ72 and other inhibitors is severalfold higher, although uncertainty in these values may approach 50%. According to eq A12a, with the same substrate, a change in C must be due to the K_I'/K_I term (Table 3), calculated with $K_S' = 0.2$ mM and $K_M = 0.065$ from Table 1. As expected, values for the ratio are higher for the short-chain inhibitors, and the absolute values of the K_I'/K_I ratio are different from those obtained from the components determined independently (Table 3). A basic assumption in the analysis is that the mimics partition into all interfaces in the same way. A departure could account for some of the variation in the calculated parameter values depending on the nature of the interface (also see below).

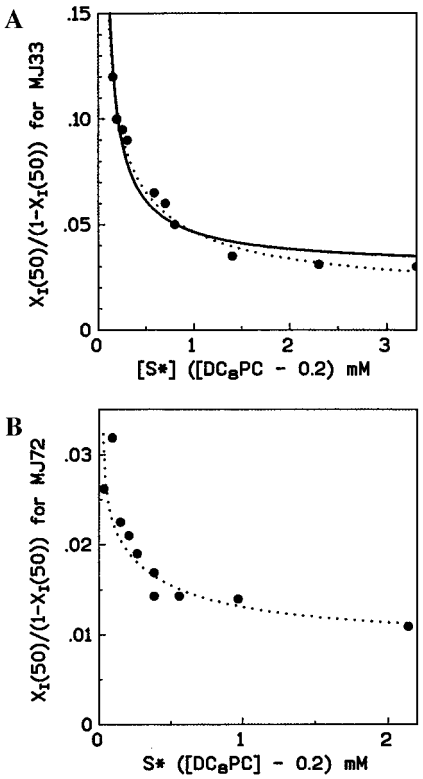

FIGURE 9: Dependence of $X_I(50)$ values for homologous competitive inhibitors on the micellar concentration of DC_8PC. The dotted curve shows the best fit to eq A12a parametrized as eq 7. (A) Inhibition by MJ33: $A = 1$ (constant), $B = 40$, and $C = 6$. The full curve fit to eq A12a was generated with independently measured $K_I^* = 0.0014$, $K_M^* = 0.04$, $K_M^{app} = 1$ mM, $K_S' = 0.2$ mM, $K_M = 0.065$ mM, $K_I' = 0.01$ mM, $K_I = 0.008$ mM. (B) Inhibition by MJ72 fitted to eq 7 to yield $A = 1$ (constant), $B = 106$, and $C = 42$. The $X_I(50)$ values are corrected for $K_I' = 0.3$ mM (Jain et al., 1993) according to eq A13b. Independently generated constants did not yield a good fit; however, as discussed in the text, they are consistent with the values of B and C. The uncertainty in the fit parameters B and C is ~30%.

K_M, but not K_M, Is Affected by NaCl*. $X_I(50)$ for MJ33 at saturating [S*] (Table 1, column 5) and its K_I^* (= 0.0014) were used to calculate K_M^* (eq A12b). The values given in Table 1 (column 6) do not change significantly with added NaCl. Equation A10 gives K_M from K_M^{app} and independently determined K_d and K_M^*. Values in Table 1 (column 4) show that K_M values decrease modestly with the chain length. The calculation of K_M in this way is based on the competitive effect that the ES state has by removing enzymes from the interface. Considering the uncertainties involved in the values of the parameters used for these calculations, it is remarkable that these values are within 50% of the values determined from the concentration dependence (Rogers et al., 1992). The effect of added NaCl on K_M is modest compared to a significantly larger effect of NaCl on K_I (Table 3) for the PC_n-ethers. If the binding modes of the ester and ether analogues are assumed to be identical, these results suggest that $K_M \gg K_S$, possibly because $k_{cat} \gg k_{-1}$ (eq A7), and the effect of added NaCl is to lower k_{-1}, without an effect on k_1 or k_{cat}. This conclusion is consistent with a lack of the effect of NaCl on V^{mono} at the cmc, which will be close to the value of k_{cat} because $K_M \ll$ cmc.

Activation Factor. According to eq A4, $K_I/K_I'K_I^*$ (Table 3, from the kinetic results of type Figure 9B) or K_d/K_d^I (Table 4, from the fluorescence measurements of type Figure 8) ratios are a measure of K_S^* type of interfacial activation factor; that is, the intrinsic affinity of the bound enzyme for the mimic increases by this factor (Jain et al., 1993b). This condition cannot be applied to K_M and K_M^* unless we are in a true quasiequilibrium. Values of activation factor by the two methods are in a narrow range, and a trend stands out: the values for the PC_n-ethers are significantly smaller than the range of 20−50 seen for the inhibitors. Unlike the ethers but like the ester group of substrate, these inhibitors contain a *sn*-2-substituent that can provide an oxygen ligand for coordination with calcium. This is entirely consistent with the idea that K_S^* activation may occur through the calcium cofactor.

Table 5: Comparison of the Interfacial Catalytic Parameters for PLA2

substrate	[NaCl]	K_M^*	k_{cat}^* (s^{-1})
$DC_{14}PM$	1 mM	0.35	400
$DC_{14}PC$	4 M	0.5	450
$DC_{14}PC$/Prod	1 mM	0.7	300
DC_8PM	1 mM	0.015	1450
DC_8PC	4 M	0.07	2350
DC_7PM	1 mM	0.05	600
DC_7PC	4 M	0.1	700
DC_6PM	1 mM	0.15	250
DC_6PC	4 M	0.25	300

The fact that the activation factors match so well is in part due to the fact that some of the possible sources of errors cancel out. Typically, individually determined constants have 30% scatter. However, measurements carried out under different conditions and at different interfaces show a wider range and a systematic bias. In addition, inhibitors have significantly different local interactions at different interfaces (Lin & Gelb, 1993), and the magnitude of the K_S^* activation may also depend on the nature of the interface. To a large extent we avoid possible difficulties by using kinetically measured K_I^* and K_I'/K_I, the rationale being, if K_I' values are different in the different interfaces, we would also expect K_I^* values to be different but in a way so that $K_I'K_I^*$ is invariant. That is, if a change in K_I' is due to a stronger interaction of I with the interface, then we expect K_I' to decrease and K_I^* to increase in roughly the same way. Of course, K_d and K_d^I could also change at the different interfaces, but possibly also in roughly the same way.

*Effect of [NaCl] on V_M^{app} Is Primarily on k_{cat}**. Collectively, results described so far show that the effect of added NaCl is consistent with the detailed balance condition (eqs 5 and 6); that is, within the 30% range of uncertainty in these parameters, the effects of NaCl on K' and K_I compensated each other, as do the effects of NaCl on K_d and K_d^I. A lack of a significant effect of added NaCl on K_I^* and K_M^* fails to account for the 20−60-fold changes observed in V_M^{app} at 4 M NaCl compared to that at 0.1 M NaCl (Table 1). Even in the extreme outer range of all the data, 0.02−0.5 mol fraction for K_M^*, the calculated value of k_{cat}^* [$= V_M^{app}(1 + K_M^*)$] would not change by more than a factor of 2. On the basis of these results, we arrive at an inescapable conclusion that the 20−60-fold increase in V_M^{app} for the DC_nPC aggregates produced by addition of 4 M NaCl is primarily due to an increase in k_{cat}^* (eq 3), or at the very least the effect is on a step after the formation of E*S (see section E in the Appendix).

Values of Interfacial Rate and Equilibrium Parameters Are Comparable in Vesicles and Micelles. Values of the catalytic parameters summarized in Table 5 were obtained by

protocols described above. These results show that K_M* and k_{cat}* for anionic DC_nPM micelles in 1 mM NaCl are virtually the same as those for zwitterionic DC_nPC micelles in 4 M NaCl. Thus, the source of anionic charge at the interface, whether induced by selective Cl^- partitioning or by the anionic head group on the substrate, makes little difference. This conclusion is consistent with independent substrate specificity results for PLA2 (Ghomashchi et al., 1991), which showed that the k_{cat}*/K_M* ratio does not change with the structure of the head group of the substrate. Also note that the equilibrium parameters determined in zwitterionic neutral diluents (Jain et al., 1991a) are completely in accord with the processive kinetic parameters in anionic aggregates obtained under a variety of conditions (Jain et al., 1995). Because such effects on the primary catalytic parameters for PLA2 are attributable to changes in the substrate structure, we conclude that these parameters are only modestly influenced by the organization of the interface.

DISCUSSION

Results reported here and elsewhere demonstrate the general usefulness of Scheme 1 for the interpretation of interfacial enzymology. The model is fully analyzed for PLA2 in two experimentally established limits at which the catalytic turnover remains rate limiting. The processive scooting mode kinetics provides a basis for establishing the primary rate and equilibrium constants with well-defined mechanistic and structural significance for PLA2 bound to anionic vesicles (Jain et al., 1986a−c, 1993b, 1995; Berg et al., 1991). In this paper we have extended the model to include the fast exchange limit seen on zwitterionic micelles. The significance of these results and the underlying assumptions are discussed in the broader context of interfacial catalysis by PLA2.

Enhanced hydrolysis of micellar DC_nPC dispersions by PLA2 has been the grail of interfacial enzymology. An apparent increase in the observed rate above the cmc is generally interpreted as interfacial activation (Verheij et al., 1981; Gelb et al., 1995; de Haas et al., 1971; Pieterson et al., 1974; Dutilh et al., 1975; Gabriel et al., 1987; Lewis et al., 1990; Roberts, 1991; Hada et al., 1993; Yuan et al., 1990; Rogers et al., 1992). Our results confirm the essence of these observations. We have developed the mechanistic significance of K_M^{app} and V_M^{app} and analyzed the apparent parameters in terms of the primary rate and equilibrium constants with well-established mechanistic significance. Contrary to earlier suggestions [reviewed in Jain and Berg (1989)], the organization of the acyl chains in the interface appears to have little effect on the catalytic parameters because hydrolysis rates are essentially the same in "disordered" micelles and "ordered" vesicles.

Previous work demonstrated that interfacial anionic charge controls the binding of PLA2 to the interface (Apitz-Castro et al., 1982; Jain et al., 1982; Jain & Berg, 1989); however, the allosteric effect of the interfacial anionic charge on k_{cat}* is an unexpected finding. The crucial conclusion that emerges from our analysis is that the negative charge density of the interface is the single most important variable for the binding of PLA2 to the interface and for k_{cat}* activation.

Catalytic Turnover Rate Is Limiting. Intermicellar exchange of short-chain phospholipid occurs via monomer exchange through the aqueous phase and by the fusion−fission mechanism (Fullington et al., 1990). On the basis of the diffusion-limited on-rate and the value of the cmc for DC_7PC, the monomer exchange rate is expected to be faster than 10^5 s^{-1} (Aniansson et al., 1976; Soltys & Roberts, 1994). Although a direct measurement of the exchange rate of substrates with enzyme-containing micelles is not possible, evidence in support of rapid exchange under our kinetic conditions (Table 1 and Figure 2) comes from several sources. The fact that V_M^{app} increases with the chain length (Table 1) suggests that the highest observed rate of 2000 s^{-1} for DC_8PC in 4 M NaCl is not limited by the replenishment rate. Under exchange-limiting conditions the rate should decrease with increasing chain length (Fullington et al., 1990). The oxy/thio element effect at V_M^{app} is consistent with the chemical step being fully rate limiting because the same magnitude of the element effect is observed in the scooting mode with WT and with mutants (Jain et al., 1992; Liu et al., 1995; Huang et al., 1996), except where the transition state may have changed (Sekar et al., 1997). In short, in the fast exchange limit, the catalytic turnover remains rate limiting for the hydrolysis of short-chain DC_nPCs, which is consistent with the pseudophase model for micelles (Tausk et al., 1974a−c; Fendler, 1982; Bunton et al., 1991).

Kinetically Uninterpretable Reaction Progress Is Predicted under Slow Replenishment Conditions. The analysis developed in this paper and elsewhere (Berg et al., 1991) cannot be used if the microscopic steady-state condition for the catalytic turnover at the interface is not satisfied. Recognizing exchange-limited kinetics is difficult, and a linear reaction progress does not necessarily assure the microscopic steady state for interfacial turnover. Sources of such misconceptions associated with commonly used assays for interfacial catalysis (see also the last section) deserve attention because at least in two cases exchange-limited kinetics results in an apparent pseudo-zero-order kinetics:

(a) In monolayers, the unstirred aqueous layer at the interface is responsible for the long pre-steady-state lag period observed during the lipolysis, and its steady-state contribution to the catalytic turnover cannot be readily analyzed (Jain & Berg, 1989).

(b) In mixed-micelles of a long-chain phospholipid with a detergent, the observed rate of hydrolysis by PLA2 is limited by the rate of substrate replenishment (Jain et al., 1993a). The fact that the detergent exchange rate is rapid in mixed micelles of phospholipid is of little consequence for determining the substrate concentration that the enzyme "sees" at the interface of a mixed micelle. What is critical is that the substrate and product exchange rate on the enzyme-containing micelle is rapid on the time scale of the intrinsic catalytic turnover rate. The replenishment rate for long-chain phospholipid in mixed micelles is expected to be, and is, exceedingly slow via the monomer exchange mechanism because their aqueous concentration is immeasurably low, in the subnanomolar range. The exchange rate for PLA2 is even slower based on the magnitudes of the rate constants for the E to E* step (Jain et al., 1988). The fusion−fission rate of micelles depends on the bulk micelle concentration and the detergent to lipid ratio (Jain et al., 1993a; Fullington et al., 1990). These processes should also give a hyperbolic dependence of the observed rate on the bulk substrate concentration, but the apparent parameters

will not have the same significance as in systems in which the microscopic steady state precedes the catalytic turnover.

Can useful mechanistic information be gained from monolayer or mixed micelle assays? These assays, in conjunction with a suitable calibration curve, are valued for their convenience [Dennis, 1983; Carman et al., 1995; however, see Yu et al. (1993) and Bayburt et al. (1995) for alternatives]. The X_I values for potent inhibitors obtained in mixed micelle assays are directly related to intrinsic K_I* (de Haas et al., 1993), albeit with the assumption that inhibitor distribution is uniform in the micelle population. However, the risk of possible artifacts, the uncertainty in the meaning of the apparent parameters, and the inability to obtain primary rate and equilibrium parameters seriously limit their general utility. In principle, it is possible to adjust the exchange parameters to account for the changing conditions with the reaction progress. Even if the chemical step remains the slowest step, the resulting relations will be far more complex than eq A5 or A6, and the apparent parameters obtained under these conditions would be difficult to reliably transform into primary parameters.

NaCl Influences K_d and k_{cat}.* Virtually no rate enhancement for the hydrolysis of DC_7PC (Figure 2B) occurs above the cmc unless the reaction mixture contains NaCl, and the maximum observed rate for DC_nPC in 4 M NaCl is comparable to that for the hydrolysis of the anionic analogues (Table 5). The conclusion that the anionic surface charge influences both K_d and k_{cat}* also relates to another observation. For example, the initial rate of hydrolysis of zwitterionic $DC_{14}PC$ vesicles is very slow until a critical mole fraction of products accumulates in enzyme-containing vesicles (Upreti & Jain, 1980; Apitz-Castro et al., 1982). Enhanced hydrolysis of zwitterionic phospholipid in the presence of anionic amphiphiles (Jain & Berg, 1989; Ghomashchi et al., 1991) can now be attributed to changes in K_d and k_{cat}*. Note that results in Table 5 rule out any significant acyl chain packing effects on the catalytic turnover; however, two related effects may have a modest contribution: (a) the local thermodynamic state of the substrate or mimic may depend on the nature of the interface and (b) the effect of charge and the phase properties on K_d is mainly due to the distribution of anionic amphiphiles in a zwitterionic matrix (Jain et al., 1989; Jain & Berg, 1989).

K_d Dominates K_M^{app} and the Effect of Added NaCl on the Interfacial Equilibria Is Compensated. The effect of added NaCl on K_M^{app} is primarily caused by the effect on K_d because selective binding of Cl^- over Na^+ makes the zwitterionic interfaces anionic. The effect of NaCl on K_M*, K_I*, and K_M is modest. Binding of PLA2 to zwitterionic interfaces at low [NaCl] is poor as shown by larger K_d (Table 4) and shorter retention times (Figure 7A). Magnitudes of the K_d(I) values (Table 4) show that the underlying K_I* values (eq 1) at zwitterionic interfaces correlate well with those derived from the kinetic parameters at anionic interfaces (Jain et al., 1991b, 1995). Also, the magnitudes of the salt effects on K_d and K_d^I are virtually the same (Figure 7), and in both cases the effect of NaCl appears to be dominated by electrostatic interactions.

There is no salt effect on K_I*. The effects on K_I and K_d are compensated by changes in K_I' and K_d^I, respectively, because added NaCl drives the hydrophobic acyl chains out of water to the more hydrophobic surface of the enzyme. Salting-out effects on amphiphiles also change micelle size (Tausk et al., 1974a−c), the rate of fusion−fission of micelles (Fullington et al., 1990; Slotys & Roberts, 1994), the phase properties of bilayers (Jain & Wu, 1977; Cunningham & Lis, 1986; Bartucci et al., 1996), and the magnitude of the solvation of the head groups (Collins & Washabaugh, 1985). To what extent such effects have a common molecular origin remains to be established.

Quasiequilibrium for the Catalytic Turnover. We have shown that the chemical step is rate limiting at V_M^{app}. According to Scheme 4, this compound parameter (eq A9) involves all the steps of the catalytic cycle in the interface:

Scheme 4

$$E^* + S^* \underset{k_{-1}^*}{\overset{k_1^*}{\rightleftharpoons}} E^*S \xrightarrow{k_2^*} E^*P \underset{k_{-3}^*}{\overset{k_3^*}{\rightleftharpoons}} E^* + P^*$$

that is, substrate−enzyme association and dissociation with rate constants k_1* and k_{-1}*, the chemical step k_2* and product−enzyme dissociation and association rate constants k_3* and k_{-3}*. The contribution of k_{-3}* is negligible when product does not stay in the interface. On the basis of the magnitude of the oxy−thio element effect, k_2* is rate limiting in k_{cat}*, which requires that $k_3^* \gg k_2^*$. In this limit $k_{cat}^* = k_2^*$ and

$$K_M^* = \frac{k_2^* + k_{-1}^*}{k_1^*} = K_S^*\left(1 + \frac{k_{cat}^*}{k_{-1}^*}\right) \qquad (8)$$

Because k_{cat}* is strongly salt dependent and K_M* and K_S* are not, the last equality on the right-hand side suggests that $k_{-1}^* \gg k_{cat}^*$, and that $K_M^* = K_S^*$. The last equality is also consistent with the observations that NaCl does not influence K_M*, the values of K_I* are within a factor of 2 of K_M*, and K_M* does not have the oxy/thio effect. Values of K_M* are <1 (Table 5) so that $k_1^* > k_{-1}^* \gg k_{cat}^*$ should hold and the chemical step must be the slow step for interfacial turnover. This differs from the results for DMPM vesicles for which $K_M^* \gg K_S^*$ and substrate release from E*S is slow, $k_{-1}^* \ll k_{cat}^*$ (Berg et al., 1991). This analysis suggests that the chain length of the substrate may have a significant influence on the magnitude of the association and dissociation rates, k_1* and k_{-1}* [see also Liu et al. (1995)].

Selective Partitioning of Anions into the Zwitterionic Interface. The NaCl-dependent increase in the binding of PLA2 to zwitterionic interfaces implies selective partitioning of anions over the cations. The results of the chemical trapping experiments show that added NaCl increases the concentration of Cl^- at the surface of zwitterionic micelles and vesicles. Thus, the surface must develop a net negative charge (Bapista et al., 1992) as shown directly by an increase in the electrophoretic mobility of $DC_{14}PC$ vesicles (Tatulian, 1983). A possible molecular basis of this effect in terms of the orientation of the phosphorus−nitrogen dipoles of phosphocholine at the interface with the cationic group toward the aqueous phase [e.g. see Hauser et al. (1981)] is unlikely because preferential anion partitioning is also seen with aggregates of sulfobetaines, in which the negative charge is probably protruded toward the aqueous phase (Bunton, 1989). Thus, $[Cl^-]$ in the interface may have its origin in ion-specific factors that favor selective partitioning.

The 10-fold decrease in K_d and K_d^I produced by increasing [NaCl] from 0 to 4 M is consistent with a role for electrostatic interactions between the interfacial recognition region of

PLA2 (i-face) and the interface. Electrostatic interactions (Honig & Nicholls, 1995; Nakamura, 1996), including those across the electrical diffuse double-layer on macromolecular surfaces (Cevc, 1990; McLaughlin, 1989), are relevant for PLA2. The binding of PLA2 involves the hydrophobic effect as well as electrostatic interactions between the cationic residues on the interfacial recognition region (i-face) of PLA2 and the anionic surface (Dijkstra et al., 1981; Ramirez & Jain, 1991; Scott et al., 1994; Zhou & Schulten, 1996). Competition between the counterion species at aggregate and protein surfaces (Bunton et al., 1991; McLaughlin, 1989; Kirchner, 1996) may account for the salt-dependent desorption of PLA2 from anionic interfaces (Jain et al., 1986c, 1991c). A 10-fold decrease in K_d and K_d^I by changing NaCl from 0 to 4 M could be an effect analogous to the salting out of the hydrophobic region of the i-face. In addition, entropic considerations suggest that PLA2 binding is accompanied by a release of anionic counterions associated with the cationic i-face of PLA2 and the release of cationic counterions from the anionic interface of the aggregate. This NaCl effect on the free energy of binding of PLA2 to interfaces is a balance of electrostatic association and the displacement of PLA2 from the anionic aggregate surface by multiple cations and anions, i.e. by ion exchange (Jain et al., 1986b, 1991c).

Low Interfacial Turnover in the Absence of the Anionic Charge and the Monomer Rate. If the interfacial anionic charge increases k_{cat}*, what is the intrinsic catalytic turnover rate at a zwitterionic interface in the absence of a net charge? An upper limit estimate is provided by results in Figure 2B where, relative to the observed rate below the cmc, the rate for micellar DC_7PC is only marginally higher. The anionic charge at the interface resulting from the (local) steady-state accumulation of fatty acid product in the enzyme-containing micelles could possibly account for a somewhat higher rate seen with DC_8PC micelles (Table 1) and the higher homologues (Apitz-Castro et al., 1982). On the basis of these observations, we assert that in the absence of any net anionic charge at the interface, the rate of hydrolysis at zwitterionic interfaces by PLA2 is about the same as the maximum rate below the cmc. Our estimate of k_{cat} with DC_7PC is $\sim 10\ s^{-1}$ obtained from the V^{mono} and K_M values in Table 1. Note that, unlike k_{cat}*, k_{cat} does not change with NaCl.

Physiological and Structural Significance. The activating effect of interfacial anionic charge on k_{cat}* may help explain the function of pancreatic PLA2 in its physiological environment, which consists of anionic mixed micelles of phospholipid with bile salts. Secreted PLA2s from other sources also show enhanced binding to anionic interfaces (Jain et al., 1991d), but the rate enhancement by increased anionic charge at the interface appears to be far less pronounced for venom enzymes (results to be published). On the other hand, the requirement for interfacial anionic charge by human inflammatory phospholipase A_2 is comparable to that of pancreatic PLA2. Several other observations are also relevant to formulating a working hypothesis for understanding such evolutionary differences in structural terms. Deletion of the 60−66 loop of porcine pancreatic PLA2 enhances the activity on zwitterionic interfaces (Kuipers et al., 1989). Deletion of the 115−123 segment at the C terminus considerably lowers the rate of hydrolysis of DC_7PC at low [NaCl], although the activity in 4 M NaCl, or with anionic substrates, is virtually the same as with wild type (Huang et al., 1996). The cationic 53 and 56 residues of pancreatic PLA2s are of interest because at low salt concentrations the rate of K56M mutant of bovine PLA2 at zwitterionic interfaces is higher compared to WT (Noel et al., 1991), but the difference is insignificant at 4 M NaCl (Yu et al., results to be published). Collectively, these observations suggest that the effect of the anionic interface on PLA2 can be attributed to specific residues on the i-face, which we are pursuing.

Interfacial Activation of Lipases. Next to PLA2s, the triglyceride hydrolases (lipases) are probably the second best structurally characterized group of interfacial enzymes. Crystal structures of some, but not all, lipases show a "lid" of about 10−20 residues covering the active site. It appears reasonable that the lid moves during the substrate binding to the enzyme at the interface (Derewenda et al., 1992; Carriere et al., 1997); however, there is no conclusive kinetic evidence for this assertion. A major difficulty is that the available assays for lipases cannot provide kinetically relevant information. For example, enhanced hydrolysis of tributyrin by lipase is seen above its solubility limit (Sarda & Desnuelle, 1958); however, a kinetic interpretation of this classical observation is not possible for a variety of reasons. A major problem with this and other lipase assays is that it is not possible to ascertain the nature of the interface where catalysis occurs. Above the solubility limit, apolar glycerides form droplets of indeterminate size, which in the commonly used assay is controlled by detergents and gum arabic. Below the solubility limit of short-chain triglycerides the problem is compounded by the fact that the surface of the reaction vessel and air bubbles formed due to stirring act as effective interfaces for catalysis. On the basis of the PLA2 experience, as a variation on the fast exchange limit, we have developed an assay suitable for determining the interfacial kinetic parameters for lipases (Berg et al., results to be published). The primary kinetic parameters obtained from this protocol do indeed provide significant mechanistic insights into the function of the "lid and hinge" by addressing questions such as the following: Are lipases turned on at interfaces? If so, what features of the interface and the enzyme control the binding of the enzyme and the interfacial catalytic turnover?

To recapitulate, Scheme 1 integrates the kinetic and mechanistic bases for interfacial catalysis. In accord with this model, enhanced activity at interfaces, commonly dubbed as interfacial activation, can be experimentally shown to be due to an increased binding of the enzyme to the interface, facilitated replenishment of the substrate, opening of the lid on the active site, and the K_S*- and k_{cat}*-allosteric activation. It now seems reasonable to expect that Scheme 1, guided by the general analysis in the Appendix, will help in developing a broader base for interfacial enzymology.

ACKNOWLEDGMENT

We thank Professor Michael Gelb (Seattle) for useful comments on the manuscript.

APPENDIX: INTERFACIAL STEADY-STATE ENZYME KINETICS WITH RAPID SUBSTRATE AND PRODUCT EXCHANGE

The kinetic model in Scheme 1 can, in principle, be analyzed in the steady state to give the rate of product

formation in the general case. First, to get a steady state under initial rate conditions it is assumed that replenishment of substrate and dissociation of product to and from the micelles is much faster than catalytic turnover. Furthermore, because all of the components are connected via binding and exchange in a set of closed loops, compositional fluxes through all of the loops will occur throughout the time course of the reaction, and the rate expression for the general case will be unwieldy. To simplify the description, we will assume that all fluxes except through the turnover steps are zero. This can be achieved in a number of ways: (a) If in the turnover branches

$$\mathrm{E} + \mathrm{S} \underset{k_{-1}}{\overset{k_1}{\rightleftharpoons}} \mathrm{ES} \xrightarrow{k_{cat}} \mathrm{E} + \mathrm{P}$$

$$\mathrm{E}^* + \mathrm{S}^* \underset{k_{-1}^*}{\overset{k_1^*}{\rightleftharpoons}} \mathrm{E}^*\mathrm{S} \xrightarrow{k_{cat}^*} \mathrm{E}^* + \mathrm{P}^*$$

the rate constants satisfy $k_{-1} \gg k_{cat}$ and $k^*_{-1} \gg k^*_{cat}$, the other branches in Scheme 1 will be automatically equilibrated at the steady state. In this case, Scheme 1 could be considered as being at quasiequilibrium. (b) If binding and dissociation of enzyme to the interface is slow across the branches where the enzyme has a ligand in the catalytic site, i.e. across EI ↔ E*I and ES ↔ E*S, the closed loops in the diagram are broken. As a consequence, there are no steady-state fluxes except through the turnover branches, and enzyme-interface binding is equilibrated across the E ↔ E* branch. Note that this does not contradict the detailed balance conditions, eqs A3 and A4 below, which are valid relations for the equilibrium constants regardless of how slow the reactions may be. In the calculations below, we will apply assumption b, allowing the ES ↔ E*S branch to be out of equilibrium. In the analysis of the results, it will be seen that assumption a is not necessarily satisfied, in which case Scheme 1 could not be considered at quasiequilibrium.

A. Equilibrium of S and I across Interfaces. Dissociation constants for substrate, K_S', and inhibitor, K_I', from the interface are given by [cf. Jain et al. (1993)]:

$$K_S' = \frac{[S_{aq}]([S^*] + [I^*])}{[S^*]} = \frac{[S_{aq}]}{X_S} = \frac{[S_{aq}]}{1 - X_I} \quad \text{(A1)}$$

$$K_I' = \frac{[I_{aq}]([S^*] + [I^*])}{[I^*]} = \frac{[I_{aq}]}{X_I} \quad \text{(A2)}$$

Here $[S_{aq}]$ and $[I_{aq}]$ indicate concentrations of monomeric S and I in the aqueous phase and [S*] and [I*] are the concentrations in the interface. (Square brackets indicate concentration in moles per liter of aqueous solution volume.) $X_I = [I^*]/([S^*] + [I^*])$ and $X_S = [S^*]/([S^*] + [I^*])$ denote the mole fractions of inhibitor and substrate, respectively, in the interface. In the absence of added inhibitor, the mole fraction of substrate in the micelle is unity, i.e. $X_S = 1$ and $K_S' = [S_{aq}] =$ cmc, and its dissociation constant, K_S', is equal to the cmc for the substrate. Similarly, the dissociation constant, K_I', equals the cmc for inhibitor in the absence of substrate. Addition of inhibitor drives binding of S so that $[S_{aq}]$ ($= K_S'(1 - X_I)$) decreases and [S*] increases correspondingly. These relations assume that mixing of S and I in the micelles is ideal, i.e., that their partitioning is independent of the composition of the interface.

The dissociation constants must also satisfy the detailed balance conditions [cf. Jain et al. (1993)]:

$$K_d K_S' K_S^* = K_d^S K_S \quad \text{(A3)}$$

$$K_d K_I' K_I^* = K_d^I K_I \quad \text{(A4)}$$

These relations further assume that binding of enzyme or enzyme−mimic complex to the interface is independent of the composition of the interface.

B. Steady-State Rate. With the assumptions discussed above, we derive the following expression for the rate of product formation per enzyme:

$$v_0^I = \frac{k_{cat}^*[S^*] + k_{cat}(1 - X_I)K_M^* K_d K_S'/K_M}{[S^*]\{1 + K_M^*(1 + X_I/K_I^*)/(1 - X_I)\} + K_d K_M^*\{1 + (1 - X_I)K_S'/K_M + X_I K_I'/K_I\}} \quad \text{(A5)}$$

[S*] in eq A5 depends on inhibitor concentration. Combining the mass balance equation, $[S_{tot}] = [S^*] + [S_{aq}]$, with eq A1 gives $[S^*] = [S_{tot}] - (1 - X_I)K_S'$. In the absence of inhibitor, eq A5 reduces to

$$v_0^0 = \frac{k_{cat}^*[S^*] + k_{cat}K_M^* K_d K_S'/K_M}{[S^*](1 + K_M^*) + K_d K_M^*(1 + K_S'/K_M)} \quad \text{(A6)}$$

where $[S^*] = [S_{tot}] - K_S' = [S_{tot}] -$ cmc.

In these expressions, k_{cat}^* and K_M^* account for all of the kinetic constants that involve reactions at the catalytic site in the interface (Berg et al., 1991) and similarly for k_{cat} and K_M in solution. The oxy−thio effect described in the main text makes it unlikely that product release from the catalytic site is rate limiting for k_{cat}^*. Therefore, k_{cat}^* corresponds to the rate of chemical transformation and the Michaelis−Menten constants, K_M and K_M^* are given by

$$K_M = K_S(1 + k_{cat}/k_{-1}) \quad \text{(A7)}$$

$$K_M^* = K_S^*(1 + k_{cat}^*/k_{-1}^*) \quad \text{(A8)}$$

where k_{-1} and k_{-1}^* are the rate constants for substrate release from the ES and E*S complexes in bulk solutions and micelles, respectively.

Rewriting eq A6 as

$$v_0^0 = \frac{V_M^{app}[S^*] + V^{mono}K_M^{app}}{[S^*] + K_M^{app}}$$

we identify

$$V_M^{app} = \frac{k_{cat}^*}{1 + K_M^*} \quad \text{(A9)}$$

$$K_M^{app} = \frac{K_d K_M^*}{1 + K_M^*}(1 + K_S'/K_M) \quad \text{(A10)}$$

$$V^{mono} = \frac{k_{cat}K_S'}{K_S' + K_M} \quad \text{(A11)}$$

These are the parameters that can be identified from curve fitting of initial rate *vs* [phospholipid], e.g. Figure 4. V^{mono}

in eq A11 is the expected Michaelis−Menten rate in the aqueous phase where the substrate concentration is $[S_{aq}] = K_S' = \text{cmc}$.

C. Dependence on the Inhibitor Concentration. From eq A5 we can calculate the mole fraction of inhibitor in the interface, $X_I(50)$, for which the observed rate is half the rate in the absence of inhibitor. Thus, setting $v_0^I = 0.5v_0^0$ produces a quadratic equation for $X_I(50)$. To simplify, we neglect the contributions from turnover in the aqueous phase as well as all terms involving X_I^2—which is reasonable for strong inhibitors where $X_I(50) \ll 1$. (At low concentrations, [S*], of interface, the requirement is $X_I(50) \ll [S^*]/K_S'$.) In this limit, the result is

$$\frac{X_I(50)}{1 - X_I(50)} \approx \frac{[S^*] + K_M^{app}}{[S^*]\frac{1 + 1/K_I^*}{1 + 1/K_M^*} + K_M^{app}\frac{K_I'/K_I - K_S'/K_M}{1 + K_S'/K_M} - K_S'\left(1 + 2\frac{K_M^{app}}{[S^*]}\right)} \quad \text{(A12a)}$$

where K_M^{app} from eq A10 has been entered. In this relation, $[S^*] = [S_{tot}] - K_S'$, corresponds to the interface concentration of substrate in the absence of inhibitor. Under conditions where all enzyme is in the interface, $[S^*] \gg K_M^{app}$, eq A12a reduces to

$$\frac{X_I(50)}{1 - X_I(50)} = \frac{1 + 1/K_M^*}{1 + 1/K_I^*} \quad \text{(A12b)}$$

The same expression holds for vesicles under scooting conditions (Berg et al., 1991). X_I denotes the mole fraction of inhibitor in the interface. However, the experimental quantity is the total concentration, $[I_{tot}] = [I^*] + [I_{aq}]$, of inhibitor added to the system. If not all inhibitor binds to the interface, X_I can be determined using the mass balance relations as

$$\frac{X_I}{1 - X_I} = \frac{[I^*]}{[S^*]} = \frac{[I_{tot}] - X_I K_I'}{[S_{tot}] - (1 - X_I)K_S'}$$

Solving for $[I_{tot}]$ as a function of X_I and $[S_{tot}]$ gives

$$[I_{tot}] = \frac{X_I}{1 - X_I}[S_{tot}] + X_I(K_I' - K_S') \quad \text{(A13a)}$$

Neglecting terms of order X_I^2, eq A13a can be rewritten for the total concentration of inhibitor, I_c^{50}, that reduces the rate by 50%

$$I_c^{50} \approx ([S^*] + K_I')\frac{XI(50)}{1 - X_I(50)} \quad \text{(A13b)}$$

where $X_I(50)$ is the mole fraction in the interface as predicted by eq A12a.

D. Determination of K_M and K_M.* Equation A12b is used to calculate K_M* when K_I* has been determined, for instance, with the protection method. Equation A10 can then be used to estimate K_M

$$K_M = \frac{K_S' K_d}{K_M^{app}(1 + 1/K_M^*) - K_d} \quad \text{(A14)}$$

where $K_S' = \text{cmc}$ (eq A1). The quantities on the right-hand side of eq A14 have been measured (Table 1). Because of the uncertainties in the experimental numbers, K_M from eq A.14 cannot be reliable unless $K_M^{app}(1 + 1/K_M^*)$ is substantially larger than K_d. Calculated values for K_M* and K_M are listed in Table 1.

E. Salt Dependence. K_M* values are independent of, wheras V_m^{app} values are strongly dependent on, added NaCl (Table 1). On the basis of eq A9 this observation implies that the catalytic rate constant, k_{cat}*, is strongly salt dependent. In a more general scheme, however, V_M^{app} includes contributions from all first-order steps after the second-order enzyme-interface binding. Stopped-flow kinetic experiments (Jain et al., 1988) have shown that enzyme-interface binding takes place in two steps, a second-order step—seemingly diffusion limited—followed by a first-order tight-binding step which makes the catalytic site available for substrates in the interface. Thus, it is possible that a salt-dependent first-order component in the E to E* step could contribute to a salt dependence of V_m^{app}. Let us consider the two-step binding scheme:

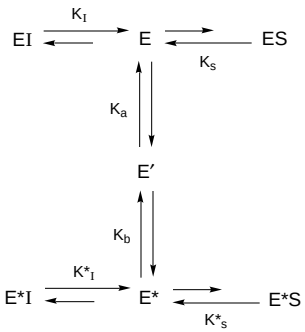

(A15)

E′ corresponds to the interface-associated state which is not catalytically active. The step with dissociation constant K_b is the first-order tight binding, which could be promoted by anionic charge at the interface. If at low salt, the interface-bound enzyme is trapped mostly in the inactive state E′, one would get a small V_M^{app} value even at saturating interface when all enzyme is interface bound. Increasing anionic charge in the interface could increase the active E* state at the expense of E′ and would increase V_M^{app}. A steady-state analysis of eq A.15, however, shows that this effect cannot give the observed salt dependence of V_M^{app}. From this scheme one finds the same results as given in eqs A5−A14 if the constants are replaced everywhere as

$$K_M^* \rightarrow K_M^*(1 + K_b),\ K_I^* \rightarrow K_I^*(1 + K_b),\ K_d \rightarrow \frac{K_a K_b}{1 + K_b} \quad \text{(A16)}$$

and the analogue of eq A9 is

$$V_M^{app} = \frac{k_{cat}^*}{1 + K_M^*(1 + K_b)} \quad \text{(A17)}$$

On the basis of eq A15, the calculated values of K_M* in Table 1 will correspond to $K_M^*(1 + K_b)$. Since these values are

independent of added NaCl, eq A17 shows that the observed salt dependence of V_M^{app} must reside in k_{cat}*.

On the basis of Scheme I, salt effects in k_{cat}* must derive from effects that appear after the formation of E*S, while effects before and including formation of E*S will show up in K_M*. Because k_{cat}* is NaCl dependent and K_M* is not, eq A8 suggests that $k_{cat}* \ll k_{-1}*$ so that $K_M* \approx K_S* = k_{-1}*/k_1*$. Since $K_M* \approx 0.1$ (Table 1), $k_{-1}* < k_1*$. Thus, $k_{cat}* \ll k_{-1}* < k_1*$ so that $k_{cat}*$ is the rate-limiting step for the hydrolysis in the interface in accordance with the oxy−thio effect discussed in the main text. Thus, hydrolysis in the interface would be at quasiequilibrium. In contrast, as discussed in the main text, the hydrolysis of monomers in the aqueous phase seems to have $K_M > K_S$ and $k_{cat} \gg k_{-1}$, so that this branch of Scheme 1 is not at quasiequilibrium.

REFERENCES

Aniansson, E. A. G., Wall, S. N., Almgren, M., Hoffman, H., Klelman, I., Ulbricht, W., Zana, R., Lang, J., & Tondre, C. (1976) *J. Phys. Chem. 80*, 905−922.

Apitz-Castro, R. J., Jain, M. K., & de Haas, G. H. (1982) *Biochim. Biophys. Acta 688*, 349−356.

Bapista, M. D. S., Cuccovia, I., Chaimovich, H., Politi, M. J., & Reed, W. F. (1992) *J. Phys. Chem. 96*, 6442−6449.

Bartucci, R., Belsito, S., & Sportelli, L. (1996) *Chem. Phys. Lipids 79*, 171−180.

Bayburt, T., Yu, B. Z., Street, I., Ghomashchi, F., Laliberte, F., Perrier, H., Wang, Z., Homan, R., Jain, M. K., & Gelb, M. H. (1995) *Anal. Biochem. 232*, 7−23.

Berg, O. G., Yu, B.-Z., Rogers, J., & Jain, M. K. (1991) *Biochemistry 30*, 7283−7297.

Bunton, C. A., Mhala, M. M., & Moffatt, J. R. (1987) *J. Org. Chem. 52*, 3832−3835.

Bunton, C. A., Mhala, M. M., & Moffatt, J. R. (1989) *J. Phys. Chem. 93*, 854−858.

Bunton, C. A., Nome, F., Quina, F., & Romsted, L. S. (1991) *Acc. Chem. Res. 24*, 357−364.

Cajal, Y., & Jain, M. K. (1997) *Biochemistry 36*, 3882−3893.

Cajal, Y., Rogers, J., Berg, O., & Jain, M. K. (1996a) *Biochemistry 35*, 299−308.

Cajal, Y., Ghanta, J., Surolia, A. K., Easwaran, E., & Jain, M. K. (1996) *Biochemistry 35*, 5684−5695.

Cajal, Y., Boggs, J., & Jain, M. K. (1997a) *Biochemistry 36*, 2566−2576.

Carman, G. M., Deems, R. A., & Dennis, E. A. (1995) *J. Biol. Chem. 270*, 18711−18714.

Carriere, F., Thirstrup, Hjorth, S., Ferrato, F., Nielson, P. F., Withers-Martinez, C., Cambillau, C., Boel, E., Thim, L., & Verger, R. (1997) *Biochemistry 36*, 239−249.

Cevc, G. (1990) *Biochim. Biophys. Acta 1031*, 311−382.

Chaudhuri, A., Loughlin, J. A., Romsted, L. S., & Yao, J. (1993) *J. Am. Chem. Soc. 115*, 8351−8361.

Collins, K. D., & Washabaugh, M. W. (1985) *Q. Rev. Biophys. 18*, 323−422.

Correia, V. R., Cuccovia, I. M., Stelmo, M., & Chaimovich, H. (1992) *J. Am. Chem. Soc. 114*, 2144−2146.

Cuccovia, I., da Silva, I. N., Chaimovich, H., & Romsted, L. S. (1997) *Langmuir 13*, 647−652.

Cunningham, B. A., & Lis, S. J. (1986) *Biochim. Biophys. Acta 861*, 237−242.

de Haas, G. H., Bonsen, P. P. M., Pieterson, W. A., & Van Deenen, L. L. M. (1971) *Biochim. Biophys. Acta 239*, 252−266.

de Haas, G. H., Dijkman, R., Lugtigeid, Dekker, N., Van den Berg, L., Egmond, M. R., & Verheij, H. M. (1993) *Biochim. Biophys. Acta 1167*, 282−288.

Dennis, E. A. (1973) *Arch. Biochem. Biophys. 158*, 485−493.

Dennis, E. A. (1983) *Enzymes 16*, 307−353.

Derewenda, U., Brzozowski, A. M., Lawson, D. M., & Derewenda, Z. S. (1992) *Biochemistry 31*, 1532−1541.

Dijkstra, B. W., Drenth, J., & Kalk, K. H. (1981) *Nature 289*, 604−606.

Dupureur, C. M., Yu, B. Z., Jain, M. K., Noel, J. P., Deng, T., Li, Y., Byeon, I. L., & Tsai, M. D. (1992a) *Biochemistry 31*, 6402−6413.

Dupureur, C. M., Yu, B. Z., Mamone, J. A., Jain, M. K., & Tsai, M. D. (1992b) *Biochemistry 31*, 10576−10583.

Dutilh, C., Van Doren, P. J., Verheul, F. E. A. M., & de Haas, G. H. (1975) *Eur. J. Biochem. 53*, 91−97.

Fendler, J. H. (1982) *Membrane Mimetic Chemistry*, Wiley-Interscience, New York.

Fullington, D. A., Shoemaker, D. G., & Nichol, J. W. (1990) *Biochemistry 29*, 879−886.

Gabriel, N. E., Agman, N. V., & Roberts, M. F. (1987) *Biochemistry 26*, 7409−7418.

Gelb, M., Jain, M. K., Hanel, A. M., & Berg, O. G. (1995) *Annu. Rev. Biochem. 64*, 653−688.

Ghomashchi, F., Yu, B.-Z., Berg, O. G., & Jain, M. K. (1991) *Biochemistry 30*, 7318−7329.

Hada, S., Fuji, S., Inoue, S., Ikeda, K., & Teshima, K. (1993) *J. Biochem. 113*, 13−18.

Hauser, H., Pascher, L., Pearson, R. H., & Sundell, S. (1981) *Biochim. Biophys. Acta 650*, 21−51.

Honig, B., & Nicholls, A. (1995) *Science 268*, 1144−1149.

Huang, B., Yu, B. Z., Rogers, J., Byeon, I. L., Sekar, K., Chen, X., Sundaralingam, M., Tsai, M. D., Jain, M. K. (1996) *Biochemistry 35*, 12164−12174.

Jain, M. K. (1973) *Curr. Topics Membr. Transport. 4*, 175−254.

Jain, M. K., & Berg, O. G. (1989) *Biochim. Biophys. Acta 1002*, 127−156.

Jain, M. K., & Cordes, E. H. (1973) *J. Membr. Biol. 14*, 101−118.

Jain, M. K., & Gelb, M. K. (1991) *Methods Enzymol. 197*, 112−125.

Jain, M. K., & Jahagirdar, D. V. (1985) *Biochim. Biophys. Acta 814*, 313−318.

Jain, M. K., & Maliwal, B. P. (1993) *Biochemistry 32*, 11838−11846.

Jain, M. K., & Rogers, J. (1989) *Biochim. Biophys. Acta 1003*, 91−97.

Jain, M. K., & Vaz, W. L. C. (1987) *Biochim. Biophys. Acta 905*, 1−8.

Jain, M. K., & Wu, N. M. (1977) *J. Membr. Biol. 34*, 157−201.

Jain, M. K., Egmond, M. R., Verheij, H. M., Apitz-Castro, R. J., Dijkman, R., & de Haas, G. H. (1982) *Biochim. Biophys. Acta 688*, 341−348.

Jain, M. K., Rogers, J., Jahagirdar, D. V., Marecek, J. F., & Ramirez, F. (1986a) *Biochim. Biophys. Acta 860*, 435−447.

Jain, M. K., Rogers, J., Marecek, J. F., Ramirez, F., & Eibl, H. (1986b) *Biochim. Biophys. Acta 860*, 462−474.

Jain, M. K., Maliwal, B. P., de Haas, G. H., & Slotboom, A. J. (1986c) *Biochim. Biophys. Acta 860*, 448−461.

Jain, M. K., Rogers, J., & de Haas, G. H. (1988) *Biochim. Biophys. Acta 940*, 51−62.

Jain, M. K., Yu, B. Z., & Kozubek, A. (1989) *Biochim. Biophys. Acta 980*, 23−32.

Jain, M. K., Yu, B.-Z., Rogers, J., Ranadive, G. N., & Berg, O. G. (1991a) *Biochemistry 30*, 7306−7317.

Jain, M. K., Tao, W., Rogers, J., Arenson, C., Eibl, H., & Yu, B.-Z. (1991b) *Biochemistry 30*, 10256−10268.

Jain, M. K., Rogers, J., Berg, O., & Gelb, M. H. (1991c) *Biochemistry 30*, 7340−7348.

Jain, M. K., Ranadive, G. N., Yu, B. Z., & Verheij, H. M. (1991d) *Biochemistry 30*, 7330−7340.

Jain, M. K., Yu, B. Z., Rogers, J., Gelb, M. H., Tsai, M. D., Hendrickson, E. K., & Hendrickson, S. (1992) *Biochemistry 31*, 7841−7847.

Jain, M. K., Rogers, J., Hendrickson, H. S., & Berg, O. G. (1993a) *Biochemistry 32*, 8360−8367.

Jain, M. K., Yu, B.-Z., & Berg, O. G. (1993b) *Biochemistry 32*, 11319−11329.

Jain, M. K., Gelb, M. H., Rogers, J., & Berg, O. G. (1995) *Methods Enzymol. 249*, 567−614.

Kirchner, S. (1996) *Biochim. Biophys. Acta 1279*, 181−189.

Kuipers, O. P., Thunnissen, M. M. G. M., de Geus, P., Dijkstra, B. W., Drenth, J., Verheij, H. M., & de Haas, G. H. (1989) *Science 244*, 82−85.

Lewis, K. A., Bian, J., Sweeney, A., & Roberts, M. F. (1990) *Biochemistry 29*, 9962−9970.

Li, Y., Yu, B. Z., Zhu, H., Jain, M. K., & Tsai, M. D. (1994) *Biochemistry 33*, 14714−14722.
Lin, H. K., & Gelb, M. H. (1993) *J. Am. Chem. Soc. 115*, 3932−3942.
Lin, T.-L., Tseng, M.-Y., Chen, S.-H., & Roberts. M. F. (1990) *J. Phys. Chem. 94*, 7239−7243.
Liu, X., Zhu, H., Huang, B., Rogers, J., Yu, B.-Z., Kumar, A., Jain, M. K., Sundaralingam, M., & Tsai, M. D. (1995) *Biochemistry 34*, 7322−7334.
Maliwal, B. P., Yu, B. Z., Szacinski, H., Squier, T., Van Binsbergen, J., Slotboom, A. J., & Jain, M. K. (1994) *Biochemistry 33*, 4509−4516.
McLaughlin, S. (1989) *Annu. Rev. Biophys. Biophys. Chem. 18*, 113−136.
Mukerjee, P. (1965) *J. Phys. Chem. 69*, 4038−4046.
Nakamura, H. (1996) *Q. Rev. Biophys. 29*, 1−90.
Nelsestuen, G. L., & Martinez, M. B. (1997) *Biochemistry 36*, 9081−9086.
Noel, J. P., Bingham, C. A., Deng, T., Dupureur, C. M., Hamilton, K. J., Jiang, R., Kwak, J., Sekharudu, C., Sundaralingam, M., & Tsai, M. D. (1991) *Biochemistry 30*, 11801−11811.
Ong, S., Liu, H., & Pidgeon, C. (1996) *J. Chromatogr. A728*, 113−128.
Pidgeon, C., & Venktarum, U. V. (1989) *Anal. Biochem. 67*, 3550−3557.
Pieterson, W. A., Vidal, J. C., Volwerk, J. J., & de Haas, G. H. (1974) *Biochemistry 13*, 1455−1460.
Ramirez, F., & Jain, M. K. (1991) *Proteins 9*, 229−239.
Roberts, M. F. (1991) *Methods Enzymol. 197*, 95−112.
Roberts, M. F., Deems, R. A., & Dennis, E. A. (1977) *Proc. Natl. Acad. Sci. U.S.A. 74*, 1950−1954.
Rogers, J., Yu, B.-Z., & Jain, M. K. (1992) *Biochemistry 31*, 6056−6062.
Rogers, J., Yu, B.-Z., Serves, S. V., Tsivgoulis, G. M., Sotiropoulos, D. N., Ioannou, P. V., & Jain, M. K. (1996) *Biochemistry 35*, 9375−9384.
Romsted, L. S., & Yao, J. (1996) *Langmuir 12*, 2425−2432.
Sarda, L., & Desnuelle, P. (1958) *Biochim. Biophys. Acta 30*, 513−521.
Scott, D. L., Mandel, A. M., Sigler, P. B., & Honig, B. (1994) *Biophys. J. 67*, 493−504.
Sekar, K., Yu, B. Z., Rogers, J., Lutton, J., Liu, X., Chen, X., Tsai, M. D., Jain, M. K., & Sundaralingam, M. (1997) *Biochemistry 36*, 3104−3114.
Soltys, C. E., & Roberts, M. F. (1994) *Biochemistry 33*, 11608−11617.
Tatulian, S. A. (1983) *Biochim. Biophys. Acta 736*, 189−195.
Tausk, R. J. M., Karmigglt, J., Oudshoorn, C., & Overbeek, J. T. G. (1974a) *Biophys. Chem. 1*, 175−183.
Tausk, R. J. M., Van Esch, J., Karmigglt, J., Voordouw, G., & Overbeek, J. T. G. (1974b) *Biophys. Chem. 2*, 53−63.
Tausk, R. J. M., Oudshoorn, C., & Overbeek, J. T. G. (1974c) *Biophys. Chem. 2*, 64−74.
Upreti, G. C., & Jain, M. K. (1980) *J. Membr. Biol. 55*, 113−121.
Verger, R., & de Haas, G. H. (1976) *Annu. Rev. Biophys. Bioeng. 5*, 77−117.
Verger, R., Mieras, M. C. E., & de Haas, G. H. (1973) *J. Biol. Chem. 248*, 4023−4034.
Verheij, H. M., Slotboom, A. J., & de Haas, G. H. (1981) *Rev. Physiol. Biochem. Pharmacol. 91*, 91−203.
Waite, M. (1987) *The Phospholipases*, Plenum, New York.
Yu, B.-Z., Berg, O. G., & Jain, M. K. (1993) *Biochemistry 32*, 6485−6492.
Yu, B. Z., Ghomashchi, Cajal, Y., Annand, R. R., Berg, O. G., Gelb, M. H., & Jain, M. K. (1997) *Biochemistry 36*, 3870−3891.
Yuan, W., Quinn, D. M., Sigler, P. B., & Gelb, M. H. (1990) *Biochemistry 29*, 6082−6094.
Zhou, F., & Schulten, K. (1996) *Proteins 25*, 12−27.

BI970855X